Electronic Thesis and Dissertation Repository

4-22-2013 12:00 AM

Cellular Adaptation of Macrophages to Anthrax Lethal Toxin-Induced Pyroptosis via Epigenetic Mechanisms

Chae Young Han
The University of Western Ontario

Supervisor
Dr. Sung O. Kim
The University of Western Ontario

Recommended Citation

CELLULAR ADAPTATION OF MACROPHAGES TO ANTHRAX LETHAL TOXIN-INDUCED PYROPTOSIS *VIA* EPIGENETIC MECHANISMS

by

CHAE YOUNG <u>HAN</u>

Graduate Program in Microbiology & Immunology

MASTER OF SCIENCE

The School of Graduate and Postdoctoral Studies
The University of Western Ontario
London, Ontario, Canada

CHAE YOUNG HAN   2013

ABSTRACT

Cellular adaptation to microbial stresses has been demonstrated in several cell types. Macrophages (MΦ) are sentinel immune cells fending off invading microbes. Anthrax lethal toxin (LeTx) is a key virulence factor released by *Bacillus anthracis* that causes rapid cell death, pyroptosis. A small number of RAW246.7 macrophages (~4%) exposed to a non-lethal dose of LeTx become resistant to LeTx-induced pyroptosis for ~ 4 weeks, termed "toxin-induced resistance (TIR)". Here, I showed that high levels of DNA methyl transferase1 (DNMT1) expression were maintained although global genomic methylation levels were not high in TIR. TIR cells treated with the DNMT inhibitor 5-azacitidine or (si)RNA targeting DNMT1 became susceptible to LeTx-induced pyroptosis. Knocking down DNMT1 also increased expression of the mitochondrial cell death proteins Bnip3 and Bnip3L involved in pyroptosis. However, DNA methylation of CpG islands in Bnip3 and Bnip3L were not different between wild type and TIR cells. Among histone modification genes examined, histone deacetylase (HDAC) 8 was up-regulated in TIR cells. The HDAC inhibitor panobinostat or siRNAs against HDAC8 rendered TIR cells sensitive to LeTx-induced pyroptosis and induced Bnip3 and Bnip3L expression. Acetylation of histone H3 lysine 27 (H3K27Ac) leads to binding of BNIP3 to H3, but this association was decreased in TIR cells. Also treatments of panobinostat or 5-azacitidine enhanced the levels of H3K27Ac in TIR cells. Collectively, these results suggest that TIR was maintained by multiple epigenetic mechanisms through up-regulating expression of DNMT1 and HDAC8. This resulted in decrease of H3K27Ac and subsequently suppressed the expression of BNIP3.

Keywords

ABBREVIATIONS

Akt	Protein Kinase B
ASC	Apoptosis-Associated Speck-like protein containing a CARD
Bacillus anthracis	B. anthracis
BAH	Two Bromo-Adjacent Homology
BMDM	Bone Marrow Derived Macrophage
BNIP3	Bcl2 Adenovirus E1B-Interacting protein 3
BNIP3L	BNIP3-Like
cAMP	Cyclic Adenosine Monophosphate
CARD	Caspase Activation and Recruitment Domain
CMG2	Cellular Receptor Capillary Morphogenesis gene 2
ChIP	Chromatin Immunoprecipitation
DMAP1	DNA Methyltransferase Associated protein 1
DNMT	DNA Methylatransferase
E.coli	Escherichia coli
EDTA	Ethylenediaminetetraacetic Acid
EdTx	Edema toxins
EF	Edema factor
ERK	Extracellular signal-Regulated Kinases
FBS	Fetal Bovine Serum
GI	Gastrointestinal
H3K27Ac	Acetylation of Histone H3 Lysine 27
HATs	Histone Acetyl Transferases
HDACs	Histone Deacetylases
HIF-1	Hypoxia-Inducible Factor 1
IL	Interleukin
IL-18	Interleukin 18
IL-1β	Interleukin-1 beta
IPTG	Isopropyl-β-D-1 thiogalactopyranoside

JNKs	c-Jun Amino Terminal Kinases
LeTx	Lethal Toxin
LF	Lethal Factor
MAPK	Mitogen Activated Protein Kinases
MBD	Methylation CpG binding domain
MECP2	Methyl CpG binding protein 2
MEK	Mitogen Activated Protein Kinase Kinases
MEKK	MEK kinases
MLN64	Metastatic Lymph Node 64 Protein
MPTP	Mitochondrial Permeability Transition Pore
NLR	NOD-like receptor
NLRP1b (NALP1b)	NOD-like Receptor & Pyrin domain –containing protein
NOD	Nucleotide Oligomerization Domain
NT	Amino-Terminus (N-terminus)
PA	Protective Antigen
PBS	Phosphate Buffered Saline
PI3K	Phosphatidylinositol 3-Kinase (PI3K)
PMSF	Phenyl Methane Sulfonyl Fluoride
qPCR	Quantitative Real Time Polymerase Chain Reaction
RFTS	Replication Foci Targeting Sequence
ROS	Reactive Oxygen Species
RTKs	Transmembrane Receptor Tyrosine Kinases
RT-PCR	Real time Polymerase Chain Reaction
SOS	Son of Sevenless
TEM8	Tumor Endothelial Marker
TIR	Toxin Induced Resistance
TNF-α	Tumor Necrosis Factor-Alpha

ACKNOWLEDGEMENTS

TABLE OF CONTENTS

LIST OF TABLES

LIST OF FIGURES

CHAPTER 1 - INTRODUCTION

1.1 Anthrax

Anthrax is an acute disease caused by the Gram positive bacterium *Bacillus anthracis (B. anthracis)*. *B. anthracis* forms a dormant endospore (referred to as spore) in harsh conditions and can be revived after decades or even centuries after forming spores[1, 2]. The spores germinate after being phagocytosed by macrophages, and toxins expressed after germination lead to a systematic immune paralysis, shock, and death[3]. Due to their stability and obnoxious nature to humans, anthrax spores have been used as a biological weapon. A recent example is the incident that occurred in the United States in 2001. Anthrax spores packaged in postal letters were sent to several news media offices and two democratic senators, resulting in 22 infections and 5 deaths[4]. In Canada, anthrax outbreaks have been reported mainly in the southern portions of Ontario and Quebec during the early 1950's. These regions were often associated with pastures contaminated by effluent from textile industries dealing with imported animal materials[5]. In 1952, introduction of federal regulations requiring disinfection of these materials greatly reduced the incidence of anthrax[6]. In 2006, there was a major outbreak in Saskatchewan[7] where dozens of farms were under quarantine and over 200 animals were affected by the disease. Anthrax can be acquired by any of three known routes: cutaneous (most frequent and less dangerous), gastrointestinal (rare) and inhalational (rare and extremely dangerous).[8]

1.1.1 Cutaneous and gastrointestinal routes

Cutaneous anthrax is caused when the spores enter through cuts on the skin, often after handling infected animal products. After deposition of spores through abrasion on the skin, spores geminate in skin tissues and local edema causes the formation of a papule that resembles a pimple[9]. Within a few days, the papules develop into fluid filled vesicles and form a painless necrotic ulcer with a black center, termed eschar. The eschar dries overtime and finally falls off, leaving a scar. Cutaneous anthrax is rarely fatal, if treated, because the infection is limited to the skin[10]. However, without treatments, about 20% of cutaneous skin infection can progress to toxemia and death.

Gastrointestinal anthrax develops a few days after ingesting spore-contaminated meat from infected animals[11]. It is generally a result of pre-existing lesions in the upper or lower gastrointestinal tract, where entry of spores and vegetation of bacteria are possible. Symptoms of an upper gastrointestinal infection can include oral or esophageal ulceration leading to the development of regional lymphadenopathy, edema, and sepsis[12, 13]. Gastrointestinal infections can be treated but usually result in fatality rates of 25~ 60%, depending upon the time of initial treatments with antibiotics.

1.1.2 Inhalation route

Inhalation of anthrax spores is considered to be extremely dangerous with a 92% mortality rate without treatments, but this can be decreased to 45% after rapid treatment with antibotics[14]. Inhaled spores are phagocytosed by alveolar macrophages or pulmonary dendritic cells, and carried to the mediastinal lymph node *via* the lymphatic system[2, 14]. Spores can remain dormant up to 60 days before germinating and, once germinated, first phase clinical symptoms including malaises, mild fever, and a mild cough are manifested. In the second phase, bacteria frequently overcomes the lymph node filter, and enter the lymphatic and blood circulation, rapidly causing massive bacteremia and toxemia[15]. This stage is accompanied by major symptoms including fever, enlarged lymph nodes, pulmonary edema with acute dyspnea (labored respiration), and cyanosis (bluish discoloration of the skin caused by poor blood oxygenation). The time course of this second phase is rapid enough such that antibiotics are no longer effective and death caused by shock is followed. It is believed that the shock is mainly caused by secreted toxins from live bacteria[15, 16].

1.1.3 Treatments & prevention

Early commencement of treatment is essential for anthrax infections because it increases chances for survival. Similar to other bacterial infections, treatments of anthrax include large doses of intravenous and oral antibiotics including fluoroquinolones, doxycycline, erythromycin, vancomycin, and penicillin. There have been many attempts to develop new drugs against anthrax since existing drugs are not effective enough if treatment is delayed. In May 2009, Human Genome Sciences submitted an application for its new

biologic drug, raxibacumab (brand name ABthrax) indicated for emergency treatment of inhaled anthrax[17]. It is a monoclonal antibody that neutralizes anthrax toxins that can cause massive and irreversible tissue injury and death. On Dec 2012, the US Food and Drug Administration (FDA) approved raxibacumab injection to treat inhalation anthrax[17].

1.2. *B. anthracis* toxins

B. anthracis produces two anthrax toxins, edema toxin (EdTx) and lethal toxin (LeTx), derived from the combination of three different factors: protective antigen (PA; 83 kDa), edema factor (EF; 89 kDa) and lethal factor (LF; 90 kDa) [18]. It has been reported that LeTx and EdTx are required for survival of spore and responsible for eventual death of infected hosts[3]. PA functions as a molecular transporter, facilitating the entry of LF and EF into cells through endocytosis. Assembly of toxin complexes begins after PA binds to cellular receptors and is cleaved into two fragments by furin-like proteases[19]. To date, two host receptors, the tumor endothelial marker (TEM8) and the cellular receptor capillary morphogenesis gene 2 (CMG2), have been identified to bind PA[20, 21]. The current model of toxin entry indicates that full length PA (83 kDa) binds to TEM8 or GCM2 and is cleaved by furin-like protease at the plasma membrane, leaving cleaved large form of PA (PA^{63}; 63 kDa) attached to the receptors. Dissociation of the cleaved 20 kDa fragment allows PA^{63} to form a spontaneous heptameric homo-oligomer that binds to EF or LF. PA^{63}-EF or –LF complexes induce a lipid raft-mediated clarthrin-dependent endocytosis[21]. Once the endosomes are acidified, the complex undergoes conformational changes, resulting in the insertion of a flexible loop of each PA molecule into the lipid bilayer and the translocation of EF and LF into the cytosol[22]. There are two virulence factors which confer pathogenicity of *B. anthracis*: a poly D-glutamic acid capsule and anthrax exotoxins[23]. These factors are encoded by two different plasmids (pXO1 & pXO2)[19, 23]. The poly-D glutamic acid capsule encoded in pXO2 whereas LeTx and EdTx are encoded by pXO1.

1.2.1. EdTx

EF is a Ca^{2+}-calmodulin-dependent adenylate cyclase that causes a prolonged increase of cytosolic cyclic adenosine monophosphate (cAMP)[24]. This is a representative example showing how bacteria can successfully evolve to disrupt a wide array of physiological processes. EF plays a crucial role in survival of anthrax bacteria in macrophages and modulation of the cytokine secreted by human monocytes. EF also collaborates with LF and PA to cause toxemia in the host, leading to death[3]. Recent studies showed that EdTx alone can cause widespread tissue damage, multi-organ failure and even death in BALB/cJ mice[24].

1.2.2. LeTx

LF is a zinc-dependent metalloprotease that cleaves the N-terminal end of mitogen activated protein kinase kinases (MEK)1 to 7, except MEK5, resulting in the inactivation of these kinases[8]. LF is composed of an N-terminal PA binding domain, a central substrate binding domain and a C-terminal catalytic domain. LeTx targets MEKs and cleaves several N-terminal acid residues of MEKs, and therefore MEKs cannot escape LF recognition through mutation without severe consequences in terms of cell physiology[25]. LeTx is the major contributor of anthrax progress in infected animals: LeTx alone can provoke various symptoms manifested in actual infections; the chemical LF inhibitors protect animal from anthrax[26].

1.3. MAPK Signaling pathway

The MAPK cascade is initiated by phosphorylations of MAPKs by the dual specific kinase MEKs. MEKs are phosphorylated and activated by MEK kinases (MEKK, e.g. Raf) that attracted to the plasma membrane by interacting with Ras superfamily GTPases[27]. MAPK signaling pathways process extracellular signals, such as environmental stresses and various cytokines, and promote various cellular functions including gene transcription. In mammals, five distinct groups of MAPKs were characterized; among them, the extracellular signal-regulated kinases (ERKs) 1 and 2,

p38 MAPKs (p38s) and c-Jun amino terminal kinases (JNKs) have been the most extensively studied[28].

1.3.1. ERK 1 &2

ERK 1 (p44) and ERK 2 (p42) play crucial roles in regulating cell proliferation, cell differentiation and cell survival. Activation of ERK is typically mediated through the transmembrane receptor tyrosine kinases (RTKs) that are activated by various cytokines and growth factors, called mitogens. Mitogens stimulate autophosphorylation of RTKs and lead to the recruitment of the guanine nucleotide exchange factor SOS (Son of sevenless). SOS promotes conversion of GDP-bound inactive to GTP-bound active RAS (GTP-Ras)[27]. GTP-Ras then interacts with the downstream serine/threonine kinase Raf (MEKK). Activated Raf phosphorylates and activates MEK1 & 2 to promote the activation of ERK1 & 2[27].

1.3.2. p38

p38 is involved in various macrophage and neutrophil functions, including respiratory burst activity, chemotaxis, granular exocytosis, adherence and apoptosis, and mediates T-cell differentiation and apoptosis by regulating gamma interferon production[29]. Four isoforms of p38 MAPK have been identified (α, β, γ and δ), and p38α and p38β are ubiquitously expressed. MEK4 represents a site of integration for the p38 and JNK pathways. While MEK6 activates all p38 isoforms, MEK3 is somewhat selective for p38α and p38β isoforms[30]. The specificity in p38 activation is initiated by the formation of functional complexes between MEK3/6 and different p38 isoforms, and the selective recognition of the activation loop of p38 isoforms by MEK3/6. Activation of p38 results from the MEK3/6-catalyzed phosphorylation of a conserved Thr-Gly-Tyr (TGY) motif in p38 activation loop[29].

1.4. LeTx and pyroptosis

1.4.1. LeTx and NOD-like receptors

LeTx causes rapid cell death of macrophages from certain strains of in-bred mice. Macrophages derived from mice including 129s/j, C3H/Hej and BALB/c undergo rapid cell death within 5 hours of LeTx exposure; whereas, macrophages derived from DBA/2, AKR, and C57BL/6 mice undergo slow apoptotic cell death, likely due to inactivation of MEKs[31, 32]. Genetic studies on these mice identified the nucleotide oligomerization domain (NOD)-like receptor & pyrin domain –containing protein (NLRP1b, Gene ID: 637517, also known as NALP1b) responsible for the rapid cell death[33]. NLRP1b is a member of the NOD-like receptor (NLR) family and is highly polymorphic. To date, five polymorphic NLRP1b alleles have been described in mice[33]. It was shown that only macrophages harboring a LeTx-sensitive allele undergo rapid cell death by LeTx.

NLRs are a family of intracellular pattern recognition receptors that recognize various microbial components and endogenous danger associated molecular patterns[34]. Upon activation, all NLRs known to date form heterogeneous multimeric oligomers, termed inflammasomes, that are composed of NLRs, pro-caspase-1 and ASC (apoptosis-associated speck-like). The multi-protein platforms facilitate auto-cleavage of pro-caspase-1 into highly active caspase-1. Caspase-1 then cleaves the proinflammatory cytokines, pro-interleukin (IL)-1 and -IL-18 into biologically active IL-1 and IL-18, respectively, and induces rapid cell death termed "pyroptosis"[35]. Inflammasomes play a role for immune cells in discriminating non-virulent and virulent pathogens[35]; in response to bacterial virulence factors including type III and IV secretion systems (T3SS and T4SS), inflammasome, NLRC4 (also known as IPAF) is activated through NLR signaling, leading to activation of caspase-1. NLRs act as an intracellular pattern recognition sensor for danger signals in the cytoplasm[36]. Among the 23 members of the NLR family in human, only several NLRs have been explored for their function and activators. Besides NLRP1 activated by LeTx, NLRP3 is activated by microbial pore forming toxins, crystalline uric acid or uric acid crystals, and extracellular ATP. NLR family CARD domain-containing protein 4 (NLRC4, also known as IPAF) senses the presence of flagellin and plays important roles in innate immune responses to gram

negative bacteria[37]. Several cellular events were commonly shown to be required for their activation, including lysosomal membrane disruption, K+ efflux and reactive oxygen species (ROS) generation[38]. However, the exact molecular mechanisms of NLR activation are largely unknown.

1.4.2. LeTx and pyroptosis

The molecular mechanism of NLRP1b activation by LeTx is yet to be defined. Several recent studies have shown that NLRP1b undergoes auto- and LF-dependent cleavages, which is required for its activation[39, 40]. It was speculated that the cleavage allows the formation of NLRP1b inflammasome through forming a caspase activation and recruitment domain (CARD) homotypic interaction with procaspase-1[41]. After NLRP1b activation, caspase-1 plays an integral role in LeTx-induced pyroptosis; however, how caspase-1 induces pyroptosis is also enigmatic[42]. Pyroptosis is a caspase-1-dependent type of cell death triggered by microbial pathogens, including anthrax lethal toxin, *Salmonella spp. Shigella spp,* and *Listeria spp*[43, 44] and various danger-associated molecular patterns. In the process of pyroptosis, DNA damage occurs and its process is caspase dependent[45]. Caspase-1 is activated during pyroptosis by a large supramolecular complex termed the pyroptosome , which is largely composed of dimers of the adaptor protein ASC (also known as an inflammasome)[46]. Pyroptosis results in the release of pathogen associated molecular patterns (PAMPs) and cytokines that activate pro-inflammatory immune cell mediators[47]. In the process of pyroptosis, cell lysis occurs upon the formation of pores in the cell membrane, which disrupts the cellular ionic gradient, leading to an increase in osmotic pressure followed by cell swelling and bursting. At the same time, the cytosolic contents release via the channels of the pores[48]. Subsequently, caspase-1 cleaves pro-inflammatory cytokines, resulting in activation. Moreover, DNA cleavage with retained integrity and nuclear condensation has been associated with the process. Several cellular events are reported to be required for LeTx-induced pyroptosis, including early mitochondrial dysfunction[49, 50] , lysosomal permeablization[51], Ca^{2+}influx [52, 53], and generation of reactive oxygen species (ROS) [54]. However, whether these events are required for caspase-1 activation or downstream of caspase-1 activation is still to be examined. We previously showed that LeTx causes

distinct characteristics of mitochondrial dysfunction from those by NLRP3, which is dependent on NLRP1b/caspase-1 and at least in part mediated through the three mitochondrial cell death genes: Bcl2 adenovirus E1B-interacting protein 3 (BNIP3) and BNIP3-like (BNIP3L) and metastatic lymph node 64 protein (MLN64)[50, 55].

1.4.3. The mitochondrial cell death proteins BNIP3 & BNIP3L

Early mitochondrial dysfunction induced by LeTx in LeTx-susceptible macrophages has been documented by us[50, 55] and others[49]. LeTx causes a loss of mitochondrial membrane potential and mitochondrial succinate dehydrogenase activity. Mitochondrial impairment and pyroptosis by LeTx requires proteasome activities, and the proteasome inhibitor MG132 prevented the mitochondrial dysfunction[49]. Our studies have also shown that LeTx causes mitochondrial dysfunction, manifested by early hyperpolarization, followed by rapid depolarization, ROS generation and depletion of free glutathione[55]. In addition, the mitochondrial cell death proteins BNIP3 and BNIP3L were also involved in the mitochondrial dysfunction. However, the molecular mechanisms of these proteins in inducing mitochondrial dysfunction are still unknown.

BNIP3 was first discovered 1994 in a yeast two hybrid screen using a B cell cDNA library as one of three novel proteins that interact with the adenovirus E1B19K protein[56]. BNIP3 predominantly localizes to the mitochondria[56, 57], where it is integrated into the mitochondrial membrane through its transmembrane N-terminal regions[56]. Previous studies suggested that BNIP3 is a weak inducer of cell death that cause loss of mitochondrial hyperpolarization, opening of the Mitochondrial Permeability Transition Pore (MPTP), and release of cytochrome c [58]. Overexpression of BNIP3 induces loss of mitochondrial membrane and cell death. However, the exact mechanism of how BNIP3 disrupts mitochondrial function is still elusive. It has been reported that BNIP3 expression is increased under hypoxic conditions and regulated by the transcription factor, hypoxia-inducible factor 1(HIF-1)[59, 60]. BNIP3 is a key regulatory gene in hypoxia-induced cell death[61, 62]. In addition, increased expression of BNIP3 leads to cell death in cardiac myocytes and other cultured cell lines. BNIP3L is a homolog of BNIP3 (also called NIX) and localizes to the nuclear envelope, endoplasmic reticulum, and

mitochondria. BNIP3L activates downstream effectors Bax/Bak through interacting with anti-apoptotic Bcl-2 and Bcl-XL[63].

BNIP3 and BNIP3L are also known to be involved in autophagy. Daido et al. first described a role for BNIP3 in autophagy in the ceramide-induced autophagic death of malignant glioma cells[64]. In these cells, ceramide induced an increase in BNIP3 expression, and BNIP3 causes mitochondrial depolarization and autophagy. In an ischemia-reperfusion model, BNIP3 induced autophagy, which protected HL-1 myocytes from cell death[65]. Similarly, hypoxia-induced BNIP3 increased autophagic death, but protected Saos2 cells from necrosis-type cell death[66]. Thus, BNIP3 and BNIP3L exhibit a dual function; they induce cell death, and they also participate in the induction of autophagy.

Expression of BNIP3 and BNIP3L was also known to be epigenetically modified in various colon carcinoma and hematopoietic cell lines. Murai et al. reported that methylation of the 5'CpG islands of BNIP3 was correlated with silencing of the gene in colon carcinoma line[67]. Treatment of BNIP3 with azacitidine restored expression of BNIP3 mRNA and protein, leading to cell death. In addition, acetylation of histone H3 in 5′ region of the BNIP3, is correlated with gene expression and inversely with DNA methylation in a hematopoietic cell line[68].

1.5. Cellular adaptation of macrophages to LeTx-induced pyroptosis

We and others showed that macrophages pre-exposed to sub-lethal doses of LeTx are refractory to subsequent high cytolytic doses of LeTx. This phenomenon is termed toxin induced resistance (TIR)[50, 69]. Salles *et al*. showed that macrophages, such as RAW 264.7 and J774A.1 cells, exposed to a low dose of LeTx become resistance to subsequent high doses of LeTx for 4 days[69]. We further showed that a small portion of TIR cells (2-4%) retain TIR characteristics for up to 5 to 6 weeks. These TIR cells show no defect in in cleaving MEKs in response to LeTx treatments, suggesting that uptake of LeTx into the cytoplasm is normal [50]. For the mechanism of TIR, an adaptive ERK activation by a

MEK-independent process or a general decrease in proteasome activity was suggested[69]. Since ERK has not yet been shown to be protective in pyroptosis, its involvement in TIR is not clear. Proteasome activity was shown to be required for LeTx-induced caspase-1 activation and pyroptosis[49]. However, we showed that TIR cells are also normal in activating NLRP1b and caspase-1 in response to LeTx, suggesting that the decrease of proteasome activity may be responsible for TIR at most in part.

A genome-wide micro-array study compared mRNAs between wild-type and TIR found that expression of BNIP3 and BNIP3L were significantly down regulated in TIR cells (Fig 1.1)[50]. Furthermore, we have shown that TIR cells are mainly resistant to NLRP1-inflammasome-induced mitochondrial dysfunction, including mitochondrial inner-membrane hyperpolarization, generation of reactive oxygen species and depletion of the anti-oxidant glutathione[55]. However, to date, how BNIP3 and BNIP3L are down regulated in TIR cells is elusive.

Fig 1.1. Sequence of cellular events involved in LeTx-induced cell cycle arrest and pyroptosis.

LF released from endosome causes mitochondrial dysfunction which requires Bnip3 and Bnip3L, resulting in cell death, known as pyroptosis. LF also cleaves MEKs, resulting in cell cycle arrest. Arrow (↑) indicates activation.
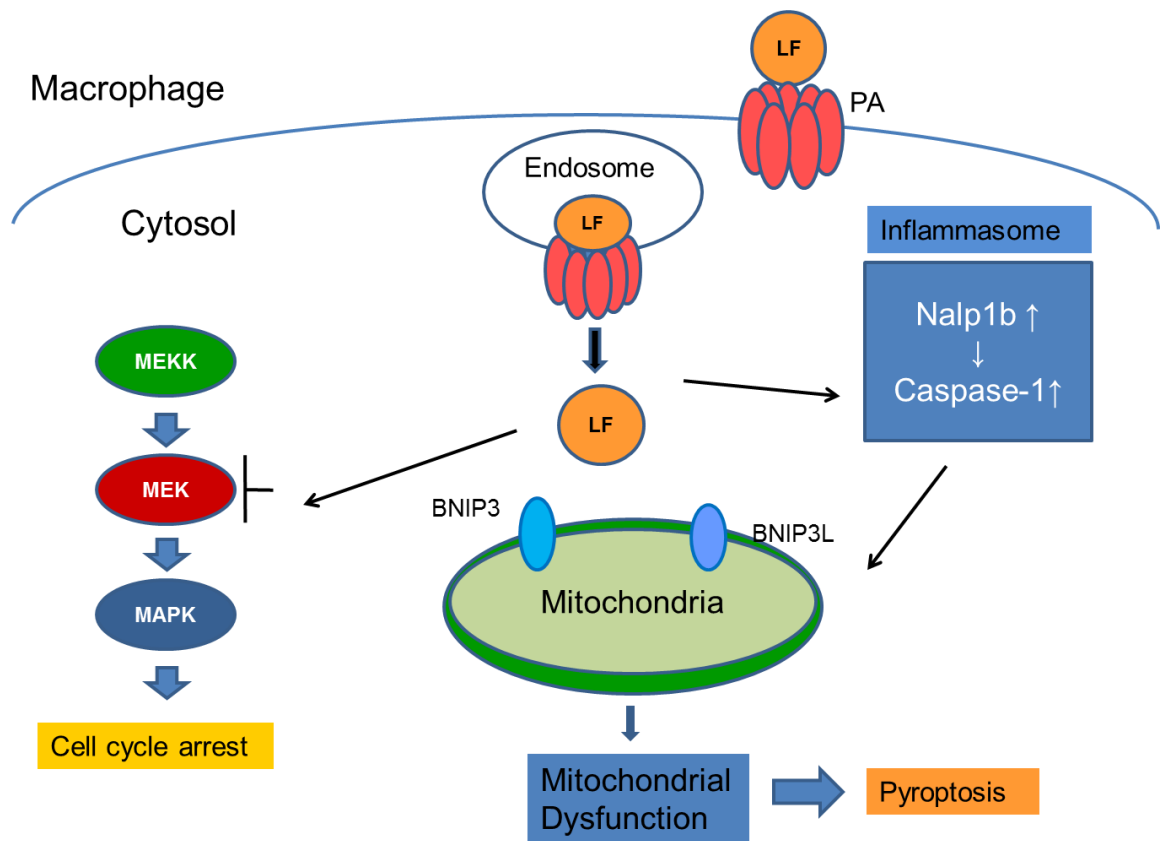
1.6. Epigenetics

The term, 'epigenetics' (epi, *επί* in Greek, means over, above or outer), literally implies 'outside conventional genetics' and is used to describe stable alteration in gene expression or cellular phenotype caused by mechanisms other than changes to the DNA nucleotide sequence[70]. DNA methylation and histone modifications are two types of epigenetic mechanisms that regulate gene expression without altering the underlying DNA sequence. Other epigenetic mechanisms such as ubiquitination, phosphorylation, and sumoylation have been studied for histone modification. Epigenetic changes may be sustained through cell divisions for the remaining life of the cell and may also last for multiple generations of cells[71].

1.6.1. DNA methylation and regulation of gene expression

DNA methylation is a mechanism which methylates cytosine residues at specific positions in the DNA molecule, resulting in repression of gene transcription[72, 73]. DNA methylation is involved in key biological processes including differentiation, imprinting, and X chromosome inactivation[70]. Failure to maintain proper DNA methylation results in developmental disorders as well as cancer[74]. CpG sites are regions of DNA where a cytosine nucleotide locates next to a guanine nucleotide in the linear sequence of bases. These sites are the main locations where most DNA methylation occurs. Methylation of CpG dinucleotide is catalyzed by DNA methyltransferases (DNMTs), which transfers the methyl moiety from the methyl donor S-adenosylmethionine to the 5' position of the cytosine ring. There are three main DNA methyltransferases (DNMTs; DNMT3a, 3b and DNMT1). DNMT3a and 3b are required for *de novo* methylation, whereas DNMT1 is involved in the maintenance of DNA methylation patterns from parental to progeny cells[75] and has a preference for methylating hemimethylated DNA [72, 76]. DNMT1 is a 195 kDa nuclear protein that harbors the DNMT catalytic domain in its C terminus and there are several regulatory domains in the N terminus, which are the DNA methyltransferase associated protein 1 (DMAP1)-binding domain, the Replication Foci Targeting Sequence (RFTS) domain, the CxxC zinc binding domain and two Bromo-Adjacent Homology (BAH) domains. Thirteen alternating repeats of Gly-Lys residues link the regulatory with the catalytic domain[77]. For repression of genes, the most critical signal is initiation of

repression by DNA itself. Methyl groups bound to the cytosine residues situated 5' to guanosines in DNA, so called CpG islands, are directly responsible for the recruitment of the HDAC complex *via* proteins such as methylated CpG binding proteins (MeCP2) and methyl CpG biding domain containing proteins (MBD), or *via* the enzymes that methylate the CpG islands, the DNA methyltransferase[78, 79].

1.6.2. Histone & Chromatin

In the nucleus, DNA is wrapped around the four core histone proteins H3, H4, H2B, and H2A to form the nucleosome which is the fundamental repeating unit of chromatin[80]. These nucleosomes are condensed into higher order structures which form chromosomes. This is required for efficient packaging of DNA into the nucleus of the cell. When DNAs are compacted into the structure, its accessibility becomes greatly limited, and this serves as a mechanism by which the cell regulates DNA mediated processes such as transcription, DNA replication, and DNA repair[81, 82]. Each histone is composed of a conserved globular histone-fold domain, and extended N and C-terminal tails. The globular domains of the histone proteins form the nucleosome core, wrapped around by 146 base pair-long DNAs. The extended histone tails protrude beyond the DNA and into the nucleoplasm. These tails serve as the sites of a variety of post-translational modifications, such as acetylation, methylation, ubiquitination and phosphorylation[81, 83]. The presence or absence of certain post-translational modifications allows localized de-condensation or condensation of the chromatin. These localized changes in chromatin structure can exert positive or negative regulatory effects on DNA-mediated processes such as gene regulation, DNA repair and DNA replication[81, 82]

1.6.3. Histone modifications and regulation of gene expression

Histones can undergo multiple post-translational modifications, which mainly occur along their N-terminal tails[82]. The histones possess polypeptide amino-terminal tails rich in positively charged lysine residues that are attracted to the negatively charged DNA. Neutralization of the positive charges by acetylation promotes gene transcription. Genome-wide studies showed that various combinations of histone modifications in a specific genomic region can lead to the activation or repression of gene expression[84]. For

example, histone methylation or acetylation can play a key role in the maintenance of both active and suppressed states of gene expression, depending on the position of methylation. It was shown that trimethylation of lysines (K) positioned on 4, 36, or 79 on H3 (H3K4me3 , H3K36me3, and H3K79me3, respectively), monomethylation of H4K20 and H2K5 (H4K20me and H2BK5me) , and acetylation of H3K9 and H3K14 result in gene activation, whereas di- or trimethylation of H3K9 (H3K9me2 and H3K9me3) and H3K27 (H3K27me3) lead to gene repression[82, 85].

1.6.3.1. Histone acetylation and gene expression regulation

Acetylation neutralizes the positively charged lysine residues of the histone N-termini, decreasing their affinity for DNA, which cause nucleosome unfolding and increases access of transcription factor to the promoter[86]. Histone acetyl transferase (HAT) is an enzyme that acetylates conserved lysine amino acids or histone proteins by transferring an acetyl group from acetyl CoA to form ε-N-acetyl (Lysine amino acid of acetyl group). It neutralizes positively charged lysine residues, leading to reduction of affinity between histone and negatively charged DNA. Also it can acetylate non histone proteins, such as transcription factors and nuclear receptors to facilitate gene expression. Increased histone acetylation by HAT is a key feature of transcriptionally active chromatin and it is also integral to the histone assembly and cell replication mechanism[80]. HATs can be largely categorized into two classes[87, 88]. Type A HATs are localized in nuclei and most likely acetylate nuclesomal histones and transcriptional activation. By contrast, type B HATs can be purified from cytoplasmic fractions, and these activities are responsible for acetylating newly synthesized histone before chromatin assembly during DNA replication[80, 87]. Most HAT associated transcriptional coactivators contain bromodomains. Bromodomains bind to acetylated lysines with ligand selectivity because of conformational differences in the loops[89]. The CBP bromodomain specifically binds acetylated Lys382 in the COOH terminus of p53, which is responsible for co-activator recruitment by p53 after DNA damage[90]. Gene expression is regulated by the balance of histone acetylation and deacetylation on lysine residues in the N-terminal tails. Disturbing the balance between HAT and HDAC may disturb gene transcription as well as DNA replication.

1.6.3.2. Histone deacetylase (HDAC)

Histone deacetylases (HDACs) are enzymes that can remove acetyl groups from a ε-N-acetyl (Lysine amino acid of acetyl group) on a histone so that histones can wrap DNA more tightly, leading to chromatin compaction and transcriptional repression[91]. Histone deacetlyation is considered to suppress the expression of several genes that regulate cell growth and differentiation. HDACs are divided into two subfamilies: the Zn^{2+} dependent HDAC class (class I, II, and IV) and NAD (Nicotinamide adenine dinucleotide)+ dependent sirtuins (SIRT; class III). Class I HDACs, which show significant homology to the yeast protein RPD3, include HDAC 1,2,3,8, and 11 that are primarily nuclear and ubiquitously expressed, whereas class II HDACs include HDAC 4, 5, 6, 7, 9, and 10 which are homologous to yeast HAD-1 like enzymes, and they are primarily localized to the cytoplasm but are known to shuttle in and out of the nucleus [91]. Class I HDACs are widely expressed and is found in most cell types, whereas class II HDACs appear to have more restricted distribution and may be involved in cellular differentiation[92, 93]. It is clearly known that HDAC enzymes usually operate along with other enzyme to silence genes. For taking these functions such as co-repression or chromatin remodeling, many proteins are recruited, result in repressor complex.

1.6.3.3. DNA methylation and histone modification inter-relationship.

Previously, several mechanisms were reported that DNMT1 and HDACs co-operatively work and induces silencing of genes[94, 95]. For example, Jones et al. suggested that methylated DNA and MeCP2 recruit HDACs, leading to gene silence[94]. Gene silencing can be caused by both histone deacetylation and methylation (Fig 1.2.), but the action of methylation is indirect and has no effect upon charge[86]. It also has been shown that methylation at a specific lysine residue (K4) in histone 3 is required for targeting histone tails for continuous acetylation and deacetylation[82]. Valeria Santini et al. also suggested that action of methyl binding proteins and histone deacetylases, and the DNA structure changes to a compact, condensed chromatin configuration, result in permanent inhibition of messenger RNA and protein production[96]. Further, hypomethylating agents and histone deacetylase inhibitors act synergistically to restore functional gene expression.

Fig 1.2. Silencing gene expression by DNA methylation and Histone deacetylation

DNA methyltransferases incorporate methyl group into cytosine residues of CpG dinucleotides. Histone deacetylases then bind to the methylated DNA and induce a closed configuration of chromatin. Transcription factors are dissociated from DNA and gene transcription is repressed[96].

Open chromatin

Condensed chromatin

Acetylated
Histone tails

Deacetylated
Histone tails

DNMT

Methylated CpG Islands

HDAC
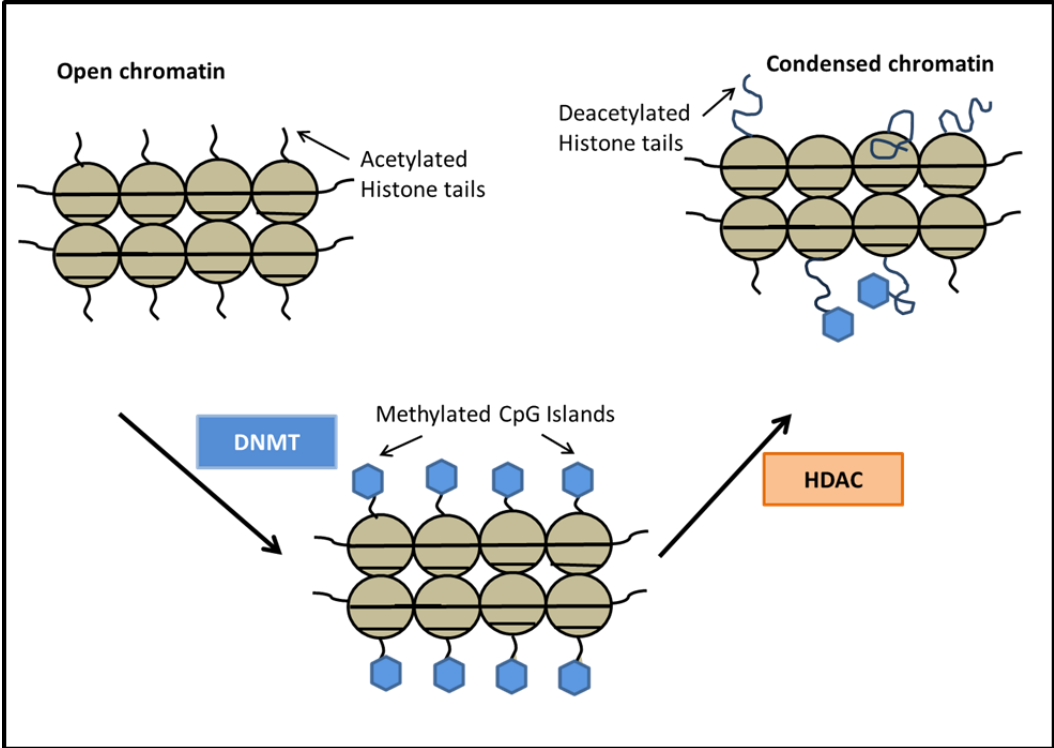
1.7. Rationale, Hypothesis and Objectives

TIR is a cellular phenomenon maintained throughout multiple cycles of cell division. Therefore, I hypothesized that TIR is mediated through epigenetic reprogramming. In order to address the hypothesis, the following objectives were proposed:

1. Examining the effects of various chemical epigenetic inhibitors on TIR

2. Examining whether specific DNA methylation and/or histone acetylation enzymes are involved in TIR

3. Examining if epigenetic reprogramming regulates expression of BNIP3 and BNIP3L in TIR cells

CHAPTER 2 - MATERIALS & METHODS

2.1. Cell culture & reagents

RAW 264.7 murine macrophages were cultured in Dulbecco's modified Eagle's medium containing 8% heated-inactivated fetal bovine serum (Sigma-Aldrich), 10 mM MEM non-essential amino acids solution, 100 units/ml penicillin G sodium, 100 µg/ml streptomycin sulfate, and 1 mM sodium pyruvate. Cells were grown at 37 ℃ in a humidified atmosphere of 5% CO_2.

Bone marrow-derived immortalized macrophages (BMDIM) from C57BL/6J mice were generated as described previously[90, 91]. Briefly, bone marrow cells were transfected with the J2 murine retrovirus, which carries the v-*raf* and v-*myc* oncogenes, and cultured for 7 days in macrophage-driving medium containing macrophage colony-stimulating factor[91]. Cells were then cultured with normal medium (RPMI 1640 medium containing 10% heat-inactivated fetal bovine serum, 10 mM MEM nonessential amino acids solution, 100 U/ml penicillin G sodium, 100 µg/mL streptomycin sulfate, and 1 mM sodium pyruvate).

TIR cells were generated as previously reported[45]. Briefly, RAW 264.7 macrophages treated with LeTx (500 ng/ml LF and 1µg/ml PA) for 5 hours, and surviving cells were plated in a fresh cell culture media . Two weeks later surviving clones were individually picked and plated on a 96-well plate. Each clone was duplicated, and tested for LeTx sensitivity, and LeTx resistant clones were pooled and propagated.

Epigenetic inhibitors used in this study were as follows. For reagents, various epigenetic inhibitors, Aza-2-deoxycytidine (Sigma,Canada), Panobinostat (Selleck,Texas), Tozasertib (LC Lab, Boston), and Anacardic acid (Santa cruz biotech, California) were obtained from indicated sources. The antibody raised againt N-terminus of MEK 1 was obtained from QED Bioscience Inc. Pan and specific antibodies raised against p38 MAPK, ERK1/2, and MEK1 (COOH terminus of MEK1) were obtained from cell signaling technologies (Pickering, Ontario, Canada). Antibody raised against H3K27Ac was purchased from Active Motif, California.

2.1.1. Epigenetic inhibitor treatment

For treatment of epigenetic inhibitors, stock solutions of Aza-2-deoxycytidine as a DNA methyl transferase inhibitor (DNMTi), Panobinostat as a Histone deacetylase inhibitor (HDACi), Tozasertib as a pan aurora protein kinase inhibitor, and Anacardic acid as a histone acetyl transferase (HAT) inhibitor were dissolved in DMSO. Wild type (RAW 264.7 macrophage cells) and TIR cells were incubated with respective inhibitors at the indicated concentration and time.

2.2. Preparation of anthrax lethal toxin

Protective antigen (PA) and lethal factor (LF) were purified as previously described[49].

Protective Antigen: PA was purified from the *E. coli* expression strain BL21 (DE3) bearing the plasmid construct (PET22B-PA). Overnight cultures were added to Luria broth containing ampicillin (50 g/mL). Cultures were grown with shaking at 37 ℃ until OD 600 of 1.0 was reached. Isopropyl β-D-1 thiogalactopyranoside (IPTG) was added to 0.5 mM, and incubated with shaking at 30 ℃ for additional 3-4 hours. Cells were harvested by centrifugation, re-suspended in a hypertonic solution with 30 mM Tris-HCl, pH 8.0, 20% sucrose, 1mm Ethylenediaminetetraacetic acid (EDTA) and incubated at room temperature for 10 min. Cells were pelleted again and resuspended in an isotonic solution with 20 mM of $MgSO_4$ and incubated on ice for 30 min.

Lethal Factor: LF was purified from *Bacillus mageterium* transformed with LF expressing plasmid (pWT-1520-LF). Overnight cultures were added to Luria broth containing tetracycline (10 mg/ml). Cultures were grown with shaking at 37 ℃ until OD 600 of 0.3 was reached. Expression of LF was induced by adding 0.5% xylose into the culture and grown for an additional 8 hours. PA containing cell lysate and LF containing culture media were precipitated with 80% $(NH4)_2SO_4$, and the precipitated proteins were pelleted by centrifugation. The pellets were resuspended in 20 mM Tris-HCl (pH8.6) with 1 mM phenylmethanesulfonylfluoride (PMSF), and dialyzed using dialysis tubing 30, 000 MWCO (Sigma). Samples were loaded onto a Q-Sepharose anion exchange column (Amersham) and proteins were isolated with an AKTA FPLC chromatography system (GE, USA). Active fractions were combined and dialyzed with PBS.

2.3. Cytotoxicity assay

RAW 264.7 macrophages cells were cultured with or without LeTx in 96-well plates for 5 hours, and 3-(4,5-dimethylthiazol-2-yl)-2,5-diphenyltetrazolium bromide was then added at a final concentration of 1 mg/mL. After incubating at 37 ℃ for additional 2 hours, culture medium was carefully aspirated, and 100 μL of dimethyl sulfoxide was added to dissolve crystals. Optical densities of the wells were analyzed using micro plate reader at 570 nm. The ratio of cell survival was estimated based on the optical density of wells by comparison with non-treated cells as 100% survival.

2.4. Total cell lysate preparation and immunoblot analysis

Total cell lysate extraction and Western blotting analysis was performed as previously described[31]. Briefly, cells were lysed in ice-cold cell lysis buffer (20 mM Tris-HCl 2 mM EGTA, 5 mM EDTA, 1 mM Na_3VO_4, 40 mM β-glycerophosphate, 30 mM sodium fluoride, 20mM sodium pyrophosphate, pH7.2) containing 1% Triton X-100, and protease inhibitor mixtures (Roche Applied Science). Cell lysates were incubated on ice for 10 min and then centrifuged at 12,500 rpm for 10 min at 4 ℃. These extracts were electrophoretically resolved in 10% SDS-PAGE gels, followed by transfer onto nitrocellulose membranes. Membranes were subsequently blocked at room temperature for 1 h with 5% (w/v) skim milk, and then incubated overnight at room temperature with antibodies. After extensive washing with TTBS (20 mM Tris pH 7.5, 150 Mm NaCl, and 0.2% Tween 20), the secondary antibody was applied at 1:40, 000 dilution and incubated for 60 min. Exposure was performed and analyzed by Odyssey fluorescence imaging system (LI-COR Inc. USA).

2.5. Quantitative Real-time PCR (qPCR)

Expression of mRNAs was quantified on a Rotor-Gene RG3000 quantitative multiplex PCR instrument (Montreal Biotech) using Express SYBR Green ER qPCR Super Master

Mix (Invitrogen). Briefly, total cellular RNA was isolated using TRIzol (Invitrogen) according to the manufacturer's instructions and then 2 µg of total RNA was reverse transcribed using oligo (dT) primers and Moloney murine leukemia virus (M-MuLV) reverse transcriptase (New England Biotechnology).The amplification mix (20 µL) contained a cDNA template derived from 1µg of total RNA, diluted to an amount of ~100 ng of cDNA, 500 nM of each specific primer set, 10 µL Express SYBR Green ER qPCR master mix with ROX (Invitrogen), which contains dNTP, SYBR Green, hot-start fast Taq polymerase and buffer and DNase-free water. The PCR conditions were as follows: 95 ℃ for 3min to activate hot start Taq polymerase, then 40 cycles of 95 ℃ for 15 sec, 58 ℃ for 30 sec,72 ℃ for 25 sec final incubation at 83℃ for 15sec. Fluorescence detection was performed immediately at the end of each annealing step.

2.6. Small interfering RNA transfection

Small interfering RNA (siRNA) oligonucleotides directed against mouse DNMT1, and HDAC8 were purchased from Qiagen. Transfection of RAW 264.7 cell with siRNA was performed with Lipofectamine RNAi Max (Invitrogen) kit according to the manufacturer's instruction. Levels of mRNA expression were confirmed by quantitative real-time PCR. Quantitative real time PCR Primers used for DNMT1, and HDAC8 are listed in Table 1.1.

2.7. Global DNA methylation analysis

Global DNA methylation was measured using the Methylamp Global DNA methylation quantification Kit (Epigentek, USA) as per the manufacturers' instructions. The kit yields accurately measures the methylcytosine content as a percentage of total cytosine content. Briefly, 200 ng of genomic DNA was purified for cell samples using DNEasy blood and tissue kit (Qiagen) and then it was added to the strip well with high affinity to the DNA and incubated for 2 hours at 37℃. The methylated fraction of DNA can be recognized by sequential incubation with 5-methylcytosine antibody for 1 hour at 37℃, and secondary antibody for 1 hour at room temperature. A colorimetric reaction allowed to quantify

DNA methylation; the quantity of methylated DNA is proportional to the optical density. Optical densities of the wells were analyzed using micro plate reader at 450 nm. A 50% methylated DNA was used as a positive control and 0% methylated DNA was used as a negative control.

$$5\text{-mC \%} = \frac{(\text{Sample OD} - \text{ME3 OD}) \div S}{(\text{ME4 OD} - \text{ME3 OD}) \times 2^* \div P} \times 100$$

2.8. Bisulfite sequencing

2.8.1. Bisulfite genomic DNA sequencing

Bisulfite treatment For bisulfite-PCR, genomic DNA was purified from wild type (RAW 264.7 macrophage) and TIR cells using DNeasy Blood & Tissue Kit (Qiagen). Genomic DNA was treated with sodium bisulfite using Epitect bisulfite kit (Qiagen) as per the manufacturer's instruction. In brief, 2 μg DNA and 140 μLEpitect bisulfite reaction buffers containing sodium bisulfite and protection buffer were mixed and modified by bisulfite mediated conversion in thermal cycler under the following condition: 99 ℃ for 5 min, 60 ℃ for 25 min; 99 ℃ for 5 min, 60 ℃ for 85 min; 99 ℃ for 5 min, 60 ℃ for 170 min. Samples were then purified using EpiTect spin column and eluted with 20 μL Buffer EB.

Bisulfite PCR, Bisulfite treated DNA was amplified using forward and reverse primers listed in Table 1.1. Bisulfite primer targeting CpG site was designed through Li lab meth primer site[92] (http://itsa. ucsf.edu/~urolab/methprimer). The PCR was performed on a thermalcycler (Stratagene, La Jolla, CA) containing 200 μM dNTPs, 2 mM $MgCl_2$, 0.3 μM forward and reverse primers and 0.5 units of *Taq* polymerase (NEB). The PCR conditions were as follows: 95 ℃ for 3 min, then 33 cycles of 95 ℃ for 1 min, 55 ℃ for 1 min and 72 ℃ for 1 min. A final incubation at 72 ℃ for 15 min concluded the PCR. PCR products were verified by gel electrophoresis and purified using gel purification.

Bisulfite sequencing For bisulfite-sequencing, the PCR products obtained with Bisulfite-PCR were cloned into PGEM-T easy vector cloning system (Promega) on LB-

Ampicillin plate. After that, 5 clones were selected and the plasmid DNA was then purified using plasmid purification system (Bioscience Inc). Purified clones are sequenced using M13 by London Regional Genomic Center (London, Ontario, CA).

2.8.2. Bisulfite pyrosequencing

Bisulfite PCR Bisulfite pyrosequencing was used for quantitative methylation analysis of the mitochondrial cell death genes, BNIP3 & BNIP3L. For preparation of samples, genomic DNA from wild type and TIR cells were isolated with DNEasy blood & tissue kit (Qiagen Cat No 69504.) and then bisulfite conversion of the genomic DNA was performed with the EpiTect Bisulfite Kit (Qiagen Cat No. 59104). Methylation states of CpG's were amplified using 20 ng of bisulfite-converted genomic DNA for two samples (wild type and TIR) and 0.2 μM of forward and reverse primers, one of which was biotinylated. PCR reactions were performed using the Pyromark PCR kit (Qiagen) optimized for bisulfite-treated DNA. PCR amplification of bisulfite-treated DNA was performed in 25 μL reactions containing 2 μL (1 U) Hot start Taq DNA polymerase (Qiagen), 2.5 μL 10X PCR buffer, 20 mM $MgCl_2$, 0.5 μl 10 mM dNTP mix, 1.0 μL (10 pmol) of each forward and reverse primers, 18 μL (~100 ng) bisulfite treated template DNA and 18 μL PCR-grade water. PCR was carried out with an initial denaturation step at 95 ℃ for 5 min, 35 cycles of 95 ℃ for 30 s, primer-specific annealing temperature (54 ℃ for BNIP3 & BNIP3L) for 30 s, elongation at 72 ℃ for 45 s and a final extension step at 72 ℃ for 5 min.

Pyrosequencing & analysis Bisulfite pyrosequencing was performed on a PyroMark Q24 Pyrosequencing System with the PyroMark Gold Q24 Reagents Kit. Pyro Q-CpG software (Biotage, Uppsala, Sweden) was used for data analysis. To demonstrate if amplification was sufficient, samples were run on QIAXcel capillary electrophoresis

2.9. Chromatin immunoprecipitation (ChIP) analysis

30 million RAW 264.7 cells were cross-linked with 1% formaldehyde and lysed in Lysis buffer [50 mM Tris at pH 8.0, 5 mM EDTA, and 1% sodium dodecyl sulfate (SDS)] supplemented with protease inhibitors (Thermo Scientific). Chromatin was sheared by sonication (Bioruptor UCD-200 ultrasound sonicator from Diagenode) for 20 mins

resulting in DNA fragments between 150 and 200 bp in size. After centrifugation to remove cell debris at 12,500 rpm for 10 mins, 5% of the sample was kept as INPUT and then diluted 10 times in dilution buffer [50 mM Tris at pH 8.0, 0.5% Triton X-100, 0.1 M NaCl, and 2 mM EDTA] supplemented with protease inhibitors. The rest of the soluble chromatin fraction was recovered and precleared for 1 hour at 4 ℃ with a mixture of Protein A and G-conjugated Dynabeads (Invitrogen). Before immunoprecipitation, 50 μL of Dynabeads protein G was incubated with 6 μg of anti-H3K27Ac antibody (Active motif, California) or -IgG rabbit antibody (Sigma) for 2 hours at 4 ℃ to evaluate the presence of nonspecific interaction. Chromatin was immnoprecipitated overnight at 4 ℃ with antibody-conjugated Dynabeads. The immunoprecipitates were extensively washed with the following combination of wash buffers (Each wash step was performed for 10 mins); high salt RIPA buffer [10 mM Tris (pH 8.0), 500 mM NaCl, 1 mM EDTA, 1% TritonX-100, 0.1% SDS, 0.1% DOC, and protease inhibitor cocktail], LiCl wash buffer [10 mM Tris-HCl (pH 8.0), 250 mM LiCl, 1 mM EDTA, 0.5% NP40, and 0.5% DOC], and TE buffer [10 mM Tris-HCl (pH 8.0) and 1 mM EDTA]. Bound chromatin and input DNA were placed in elution buffer [10 mM Tris (pH 8.0), 5 mM EDTA, 300mM NaCl, and 0.5% SDS] and, heated overnight at 65 ℃ to reverse the cross-linking. After proteinase K digestion (100 μg, 1 hour at 50 ℃), DNA fragments were purified on QIAquick Spin columns (Qiagen) in 50 μL of EB (elution buffer) and then 1 μL of that was used in each quantitative real-time PCR analysis. Sequences of promoter-specific primers are available in listed table 1.1. Sequences of primers were designed to specifically amplify proximal promoter regions from the genes BNIP3 and BNIP3L. Data are presented as enrichment of the precipitated target sequence as compared to input DNA.

2.10. Statistical analysis

Data are presented as Mean $\pm$ SE. Statistically significant differences were determined by unpaired student t-test using GraphPad software.

Table 1.1. List of primer sequences

Gene	Gene	Primer sequence (5'→ 3')
Bisulfite-sequencing	BNIP3	F:5'-TGAAGTTAGGTTGGAGGTGGGTAGA-3' R:5'-AACAAAAAAAACAAACTCAACACCCAAAAC-3'
Real time PCR	BNIP3	F:5′-GCTCCCAGACACCACAAGAT-3′ R:5′-TGAGAGTAGCTGTGCGCTTC-3′
	BNIP3L	F:5′-CCTCGTCTTCCATCCACAAT-3′ R:5′-GTCCCTGCTGGTATGCATCT-3′
	DNMT1	F:5'-AAGAATGGTGTTGTCTACCGAC-3' R:5'-CATCCAGGTTGCTCCCCTTG-3'
	DNMT3a	F:5'-ATGTGGTTCGGAGATGGCAAG-3' R: 5' AGATGGCTTTGCGGTACATGG-3'
	DNMT3b	F: 5'-CCTGTGGAGTTTCCGGCTAC-3' R: 5'- GACGCTCTTAGGTGTCACTTC-3'
	HDAC1	F: 5'-TGAAGCCTCACCGAATCCG -3' R: 5'-GGGCGAATAGAACGCAGGA-3'
	HDAC2	F: 5'-GGAGGAGGCTACACAATCCG-3' R: 5'-TCTGGAGTGTTCTGGTTTGTCA-3'
	HDAC5	F: 5'-AGCACCGAGGTAAAGCTGAG-3' R: 5'-GAACTCTGGTCCAAAGAAGCG-3'
	HDAC8	F: 5'-ACGGGAAGTGTAAAGTAGCCA-3' R: 5'-TCCACGTAGAGAATACGGTCAAA-3'
	HDAC9	F: 5'-GAGAGGCATCGCAGAGAGC-3' R: 5'-CCCACGGAATGATTCTTTCCA-3'
	GAPDH	F: 5′-GCATTGTGGAAGGGCTCATG-3′ R: 5′-TTGCTGTTGAAGTCGCAGGAG-3
ChIP	BNIP3	F: 5'-AATCTGTCCCTCAACGGCTG-3' R: 5'-GTTGGTAGATGCACCAGGCT-3'
	BNIP3L	F: 5'-TCTTCCTCCAGTCCTACCCA-3' R: 5'-CCTGGGACAGTGTTAGCCTC-3'
	GAPDH	F:5′-GCTGACATCAACTCCCAGGT-3′ R:5′-TTCCGTTCTCAGCCTTGACT-3′

CHAPTER 3 - RESULTS

3.1 Obtaining and characterizing TIR macrophages.

3.1.1. Obtaining TIR macrophages.

Although RAW 264.7 macrophages underwent cell death (~98%) by LeTx (500 ng/ml LF and 1μg/ml PA for 24 h), a small population of the surviving macrophages (~4%) remained resistant even after 6 weeks of the initial LeTx treatment. Based on MTT assays, LeTx caused ~70% of cell death in wild type cells, but less than 20% in TIR cells in 5 hours (Fig 3.1A). Cell death detected by LeTx was likely a pryroptotic cell death, since cell death was prevented by knocking down caspase-1 (Fig. 3.1B).

3.1.2. TIR cell has no defects in intracellular incorporation of LeTx.

To further examine if TIR cells had no defects in incorporating LeTx into the cytoplasm, we examined MEK1 cleavage and basal ERK and p38 activities inactivation in both wild type and TIR cells exposed to LeTx for 3 hours (250ng/ml LF & 500ng/ml PA). There was no apparent defect in MEK1 cleavage and dephosphorylation of ERK1 and 2, and p38 in TIR cells when compared with wild type cells (Fig 3.2). Since LeTx inhibited MEK cleavage leading to inhibition of the MAPK signaling cascade, cleavage of MEK1 and basal ERK and p38 indicates that TIR cells have no defects in intracellular incorporation of LeTx.

Fig 3.1. TIR cells are resistant to LeTx-induced pyroptosis.

(A) Both wild type (RAW 264.7 macrophage) and TIR cells were exposed to LeTx (LF 500ng /ml,1μg/ml PA) for 5 hours. Then cell death was measured using MTT assay. (B) Wild type cells were transfected with scrambled siRNA or siRNA targeting caspase-1 (si-CASP1) for 48 hours. Cells were then treated with LeTx (500ng/ml LF and 1μg/ml PA) for 5 hours and cell death was measured by MTT assay. Data are expressed as means and SD (n=3), * P≤ 0.05, **P≤0.01, and *** P≤0.005.
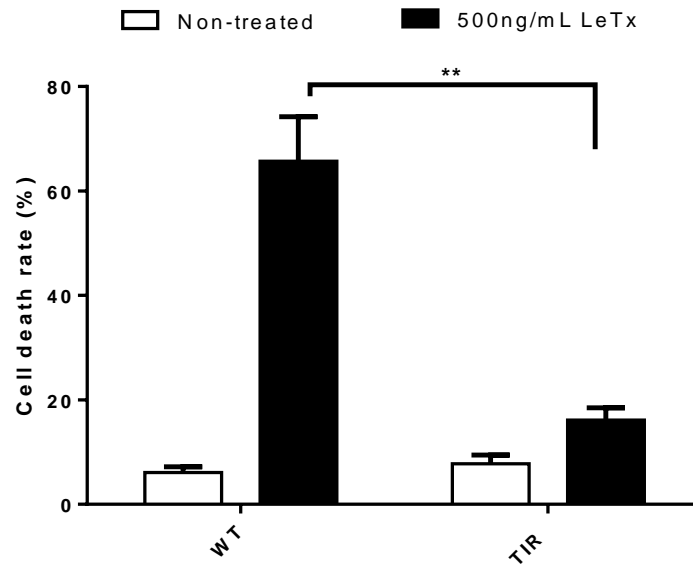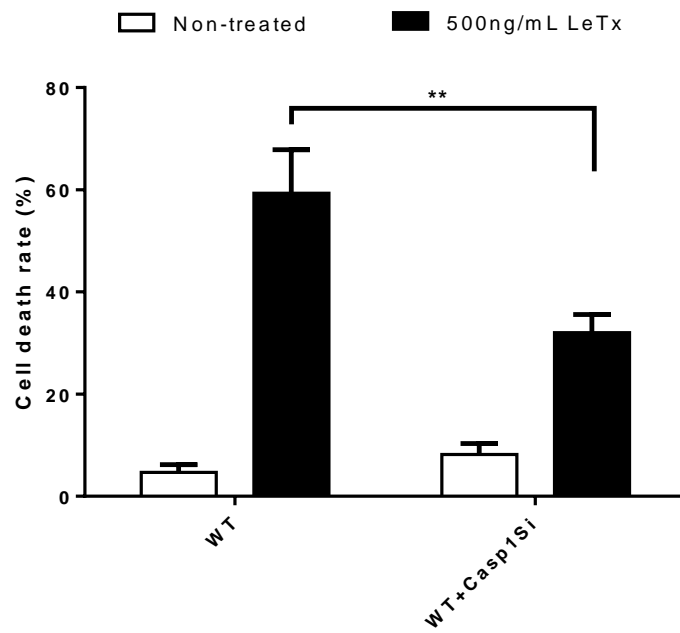
Fig 3.2. TIR cell has no defects in incorporating LeTx into the cytoplasm.
Wild type (RAW 264.7 macrophage) and TIR cells were exposed to LeTx (250ng of LF
& 500ng of PA) for 3 hours. MEK N-terminal cleavage and phosphorylation of ERK1/2
and p38 were analyzed using immunoblots. p38 was used as loading control. Data are
representative of two independent experiments.

	Wild type		TIR	
LeTx	−	+	−	+
MEK-1NT				
pERK1/2				
ERK1/2				
pp38				
p38				
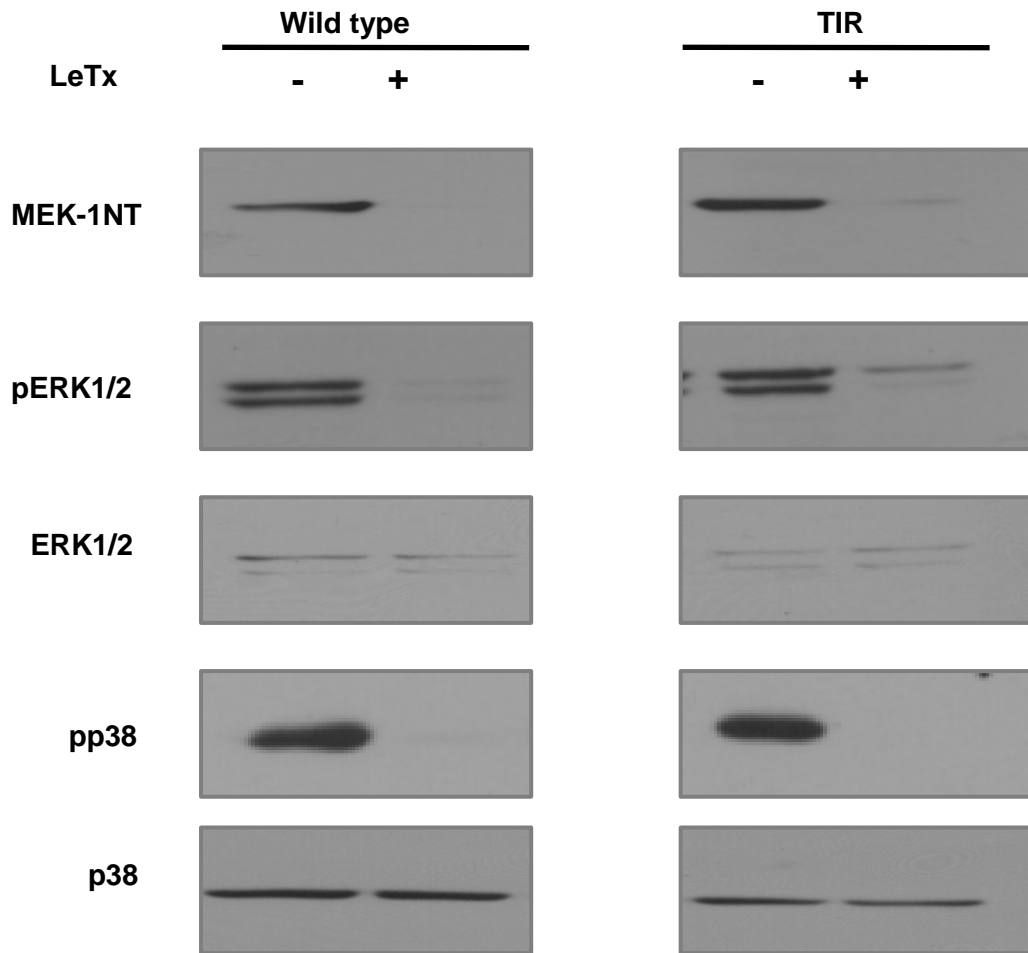
3.2. TIR is mediated through an epigenetic mechanism(s).

3.2.1. Inhibition of DNMT or HDAC sensitizes TIR cells to LeTx-induced pyroptosis.

Based on the observation that TIR was a phenomenon sustained for 6 weeks after initial treatments (~42 cycles of cell division), it is possible that an epigenetic mechanism(s) is involved in the TIR process. To examine its involvement, wild-type and TIR cells were treated with various chemical inhibitors targeting enzymes involved in epigenetic reprogramming processes: tozasertib (broad spectrum aurora kinase inhibitor, 50nM), azacitidine (broad spectrum DNA methylasetransferase inhibitor, 2.0μM), panobionstat (LBH-589, broad spectrum histone deacetylase inhibitor, 100nM), mocetinonstat (histone deacetylase inhibitor targeting HDAC1, 2, & 3: 50nM), and anacardic acid (broad spectrum histone acetyltransferase inhibitor 2.0μM) for 24 hours. Different doses of each epigenetic inhibitors were decided based on dose dependent study (Fig 3.3D). Cells were then exposed to LeTx (500ng/ml LF & 1μg/ml PA) for 5 hours and cell death was measured using MTT assay. Among the inhibitors examined, azacitidine and panobinostat significantly rendered TIR cells sensitive to LeTx-induced pyroptosis (Fig 3.3A).These results suggest that DNA methylation and histone deacetylation are involved in TIR. Of note, mocetinostat had no effects on TIR, suggesting that HDAC 1, 2, and 3 may not be involved in TIR maintenance. Furthermore, TIR cells were pretreated with azacitidine for various time points and sensitivity to LeTx was examined. As shown in Fig 3.3B, TIR cells became sensitive to LeTx in a time-dependent manner, completely regaining sensitivity to a similar level of wild-type cells in 48 hours. Panobinostat rendered TIR cells sensitive to LeTx in a dose-dependent manner and full LeTx sensitivity was reached at 100 nM concentration (Fig 3.3C).

### 3.2.2.   LeTx induces global methylation in macrophages.

Since the DNA methyltransferase inhibitor, azacitidine sensitized TIR cells to LeTx-induced pryoptosis (Fig. 3.3A and B), I first examined whether LeTx induces global DNA methylation in macrophages. The levels of global methylation were measured using

an ELISA (Enzyme linked immunosorbent assay) with antibody raised against methylated CpG dinucleotide. Genomic DNAs were added to a specifically designed well for high affinity to DNA and anti-body for CpG dinucleotide and secondary antibody were subsequently added to read methylation level through optical density (O.D.). The lowered concentration of LeTx (100ng/ml LF and 200ng/ml PA) for global methylation is treated because high concentration of LeTx (500ng/ml LF and 1μg/ml) is cytotoxic dose and therefore it can kill most cells within 24hours. Wild type cells showed a very low level of global DNA methylation (~1%), which was substantially increased (~11%) in response to LeTx in a time-dependent manner (100ng LF/ml and 200ng PA/ml; Fig. 3.4A). The global DNA methylation was decreased in azacitidine-treated samples, suggesting a role of DNA methyltransferases in the process. However, the increase of global DNA methylation was not maintained in TIR cells (Fig. 3.4C), also suggesting that global DNA methylation *per se* was not responsible for TIR. To examine the involvement of NLRP1b in global DNA methylation, macrophages originating from C57BL/6 mice harboring non-functional NLRP1b were treated with LeTx and global DNA methylation was analyzed. The macrophages showed higher levels of basal DNA methylation, which was further increased by LeTx (Fig. 3.4D). These results suggest that LeTx increased global DNA methylation independent of NLRP1b/caspase-1.

Fig 3.3. The DNMT and HDAC inhibitors sensitize TIR cells to LeTx-induced pyroptosis.

(A) TIR cells were pretreated with 50nM tozasertib, 100nM panobinostat, or 2.0 μM azacitidine, 50nM Mocetinostat, and 2.0μm Anacardic acid for 24 hours. The inhibitor doses were determined based on both dose-dependent studies with RAW 264.7 macrophage cells and IC values reported in literatures[97-99]. Non-treated wild type (WT; RAW 264.7 macrophage), non-treated TIR or pre-treated TIR cells were newly seeded on 96 plates and exposed to LeTx (500ng/ml LF and 1μg/ml PA) for 5 hours. (B) TIR cells were cultured in the presence or absence of azactidine (2 μM) for the times indicated. Non-treated WT, TIR or azacitinde pretreated TIR cells were exposed to LeTx (500ng/ml LF and 1mg/ml PA) for 5 hours. (C) TIR cells were cultured in the presence or absence of panobinostat for doses indicated overnight. Non-treated WT, TIR, or pretreated TIR cells were exposed to LeTx (500ng/ml LF and 1μg/PA) for 5 hours (D) For dose dependent studies, TIR cells were cultured in the presence and absence of varied epigenetic inhibitors including Azacitidine, Anacardic Acid, Mocetinostat, and Tozasertib followed by LeTx (500ng/ml LF and 1μg/PA) for 5 hours. (A-D) Cell death was measured using MTT assay. Data are expressed as means and SD (n=3), * P≤ 0.05, **P≤0.01, and *** P≤0.005.
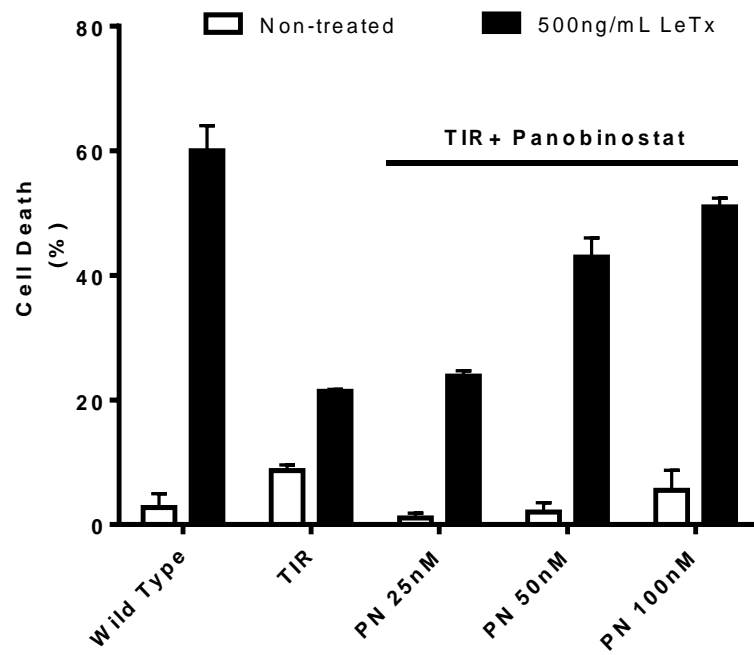
A)
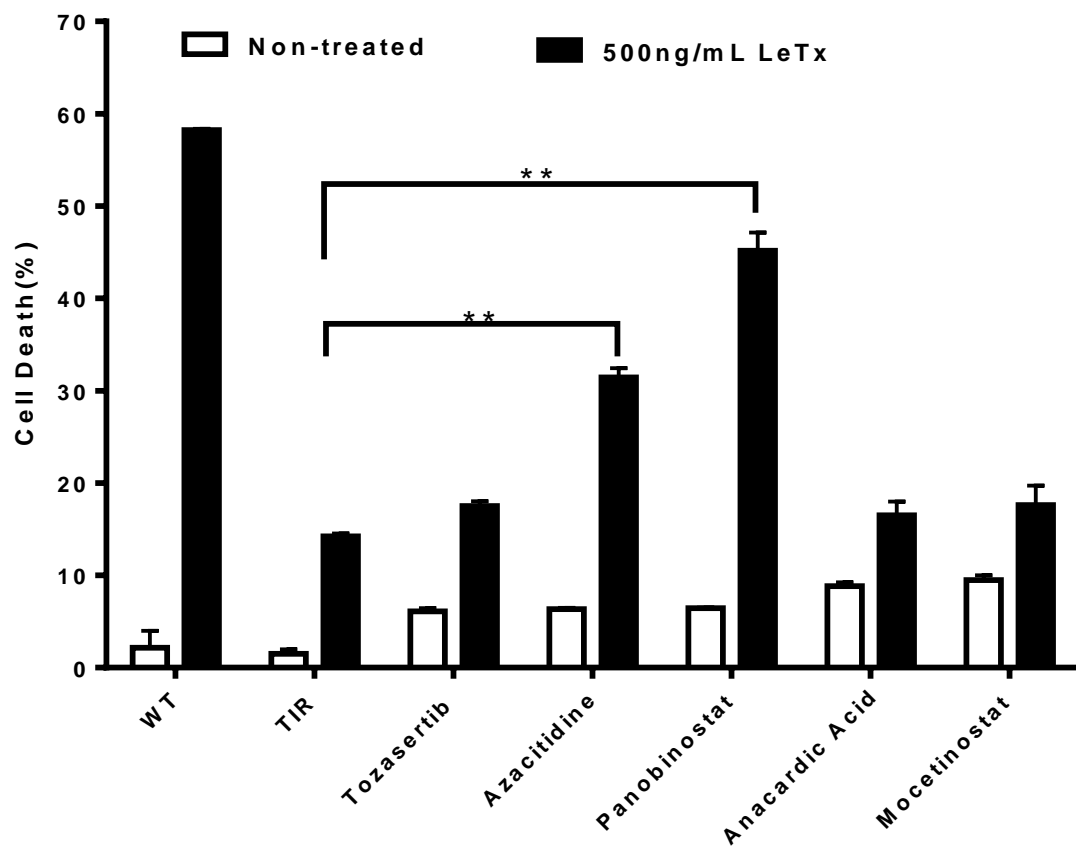
B)
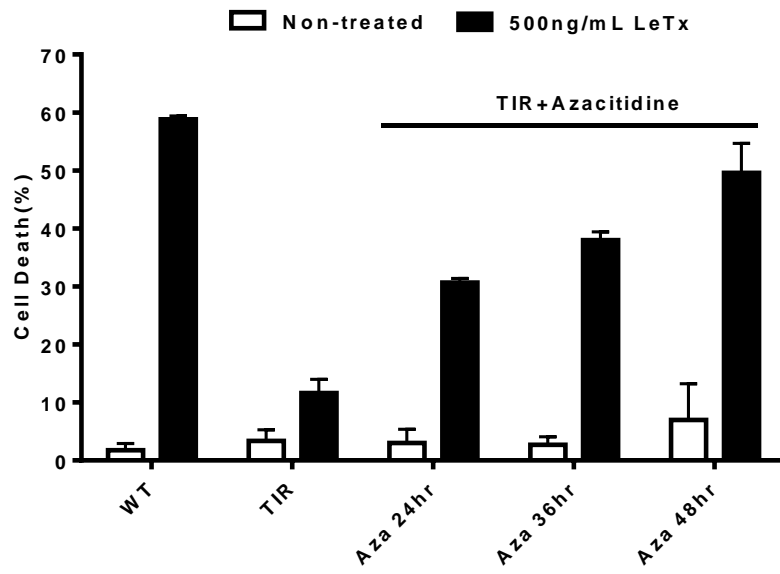
C)

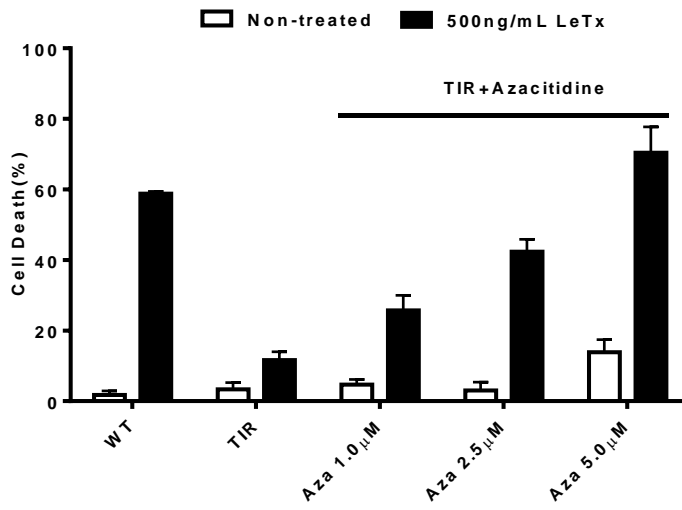# D) Dose dependent study
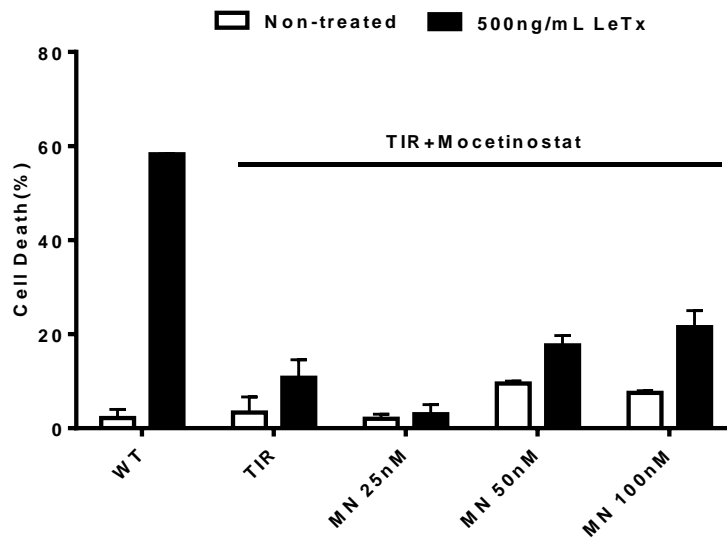
I. Azacitidine

II. Mocetinostat

III. Anacardic Acid
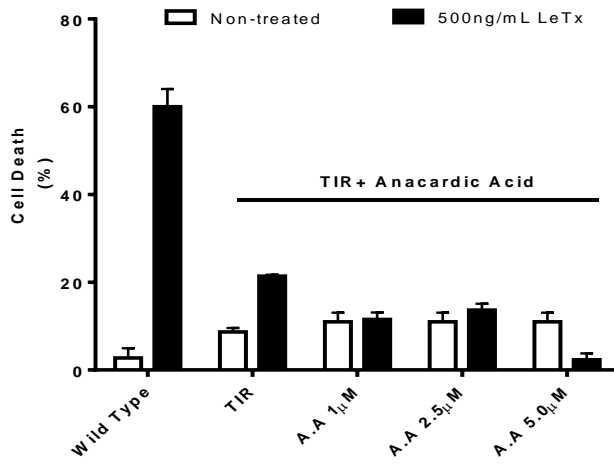
IV. Tozasertib
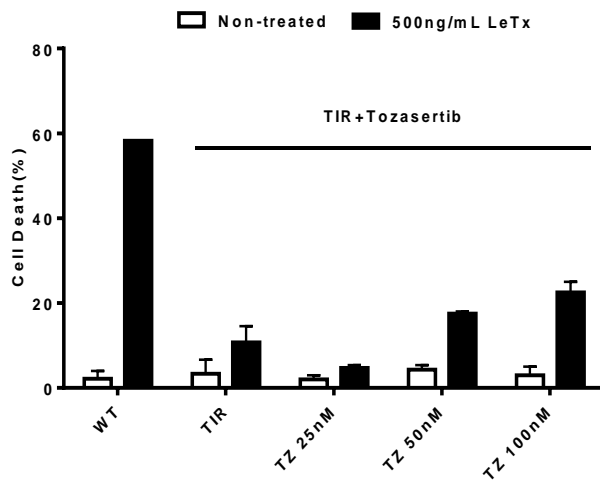
Fig 3.4. Global DNA methylation levels in TIR were not different from those of wild type cells.

(A) Genomic DNA was purified from wild type cells (WT: RAW 264. 7 macrophages) and wild type cells treated with LeTx (100ng/ml LF & 200ng/ml PA) for times indicated. (B) Genomic DNA was purified from wild type and wild type treated with LeTx (100ng LF/ml & 200ng PA/ml) for 24 hours, and wild type treated toxin for 24 hours and subsequently treated with 2.0μM azacitidine overnight. (C) Genomic DNA was purified from wild type and TIR cells. (D) Genomic DNA was purified from macrophages prepared from C57BL/6 mice (C57 cells) and C57 cells treated with LeTx (100ng/ml LF & 200ng/ml PA) for 24 hours. (A-D) Global methylation levels were measured using global methylation ELISA kit (Epigentek, USA), following the protocol provided by the manufacturer. Data are expressed as means and SD (n=3), * P≤ 0.05, **P≤0.01, and *** P≤0.005 (student's t-test).

A)

B)

42
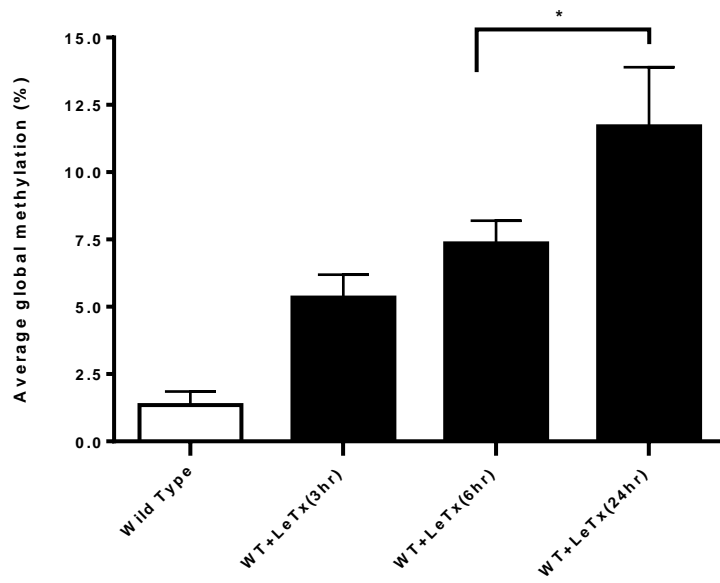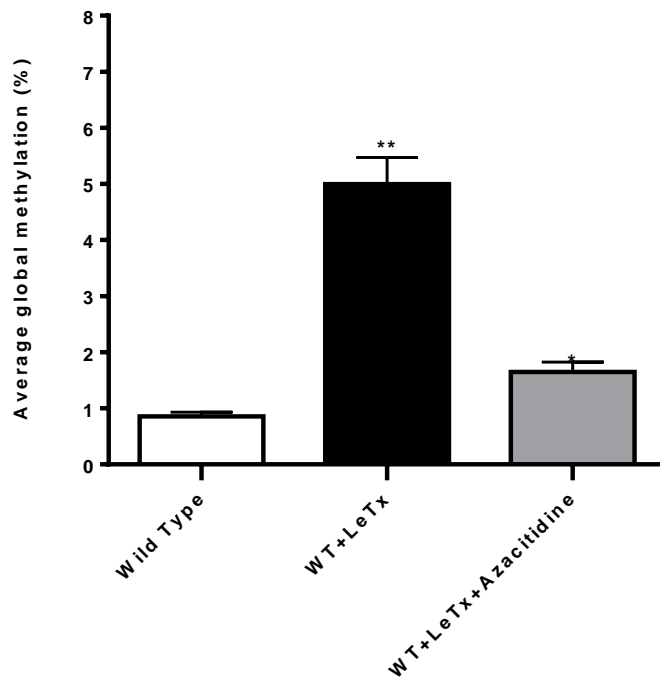
C)
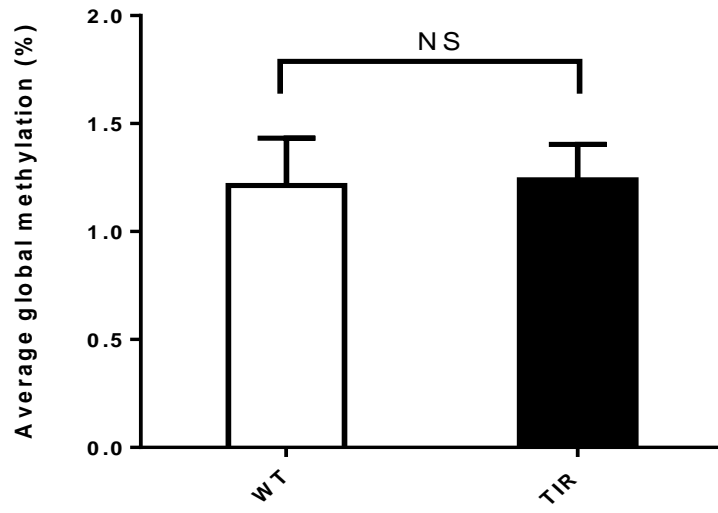
D)
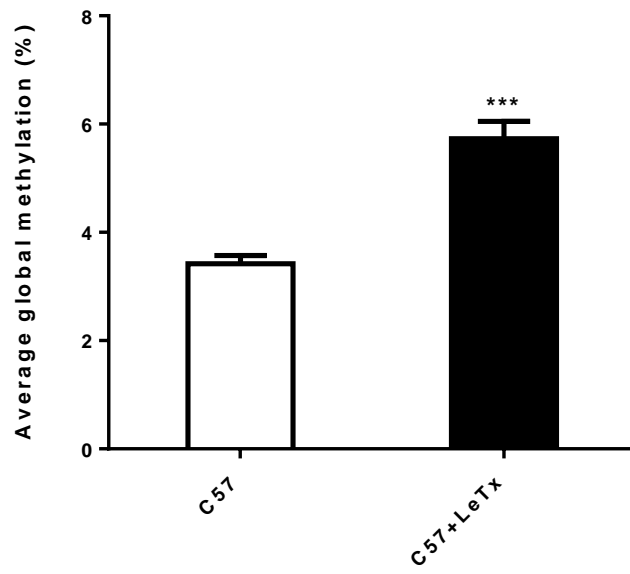
3.2.3. DNMT1 is involved in the maintenance of TIR.

Although global DNA methylation was not found to be related to TIR, DNA methyltransferase (DNMT) activity was required for maintaining TIR (Fig 3.3). To identify specific DNMTs involved in TIR, expression of DNMT1, DNMT3a, and DNMT3b was analyzed using real-time quantitative PCR (qPCR) analysis. As shown in Fig 3.5A, expression of DNMT1 was higher than 2-fold in TIR cells than wild type cells, but no significant changes were detected in the levels of DNMT3a and rather a slight but significant decrease of DNMT3b. Also, wild type cells were pretreated with LeTx for various time points, and mRNA levels of DNMT1 were examined. As shown in Fig 3.5B, mRNA of DNMT1 was increased in a time-dependent manner, suggesting that LeTx caused increase of DNMT1 and DNA methylation. These results suggest that DNMT1 played a key role in TIR. To further confirm that the correlation between DNMT1 expression and TIR, multiple TIR and wild type cell clones were examined for DNMT1 expression. Consistent with the notion, expression of DNMT1 was closely related with cell death resistance by LeTx with correlation coefficient (R^2=0.8) as shown in Fig 3.6. To functionally validate the role of DNMT1 in TIR, DNMT1 was knocked down using DNMT1-specific siRNAs in TIR cells (Fig 3.7A). DNMT1-specific but not scrambled si-RNAs knocked down about 60% of DNMT1 mRNAs (Fig 3.7A) and sensitized TIR cells to LeTx (Fig. 3.7B). Global methylation was measured using genomic DNA purified from DNMT1 specific knocked down wild type followed by LeTx treatment for 24 hours. Though LeTx-treated wild type showed a 5 fold increase in global methylation level, knock down of DNMT1 did not show an increase of methylation, suggesting that DNMT1 plays a role in global methylation induced by LeTx (Fig 3.7C).

Fig 3.5. DNMT1 is up-regulated in TIR.

(A) mRNAs from wild Type (RAW 264.7 macrophage) and TIR cells were collected and analyzed for the expression of DNMT1, DNMT3a, and DNMT3b, relative to GAPDH by quantitative real-time PCR. (B) mRNAs from wild type (RAW 264. 7 macrophage) and wild type treated with LeTx (100ng LF & 200ng PA) for times indicated were collected and analyzed for DNMT1 mRNA levels. Data are expressed as means and SD (n=3), * P≤ 0.05, **P≤0.01, and *** P≤0.005 (student's t-test).

A)

B)

47
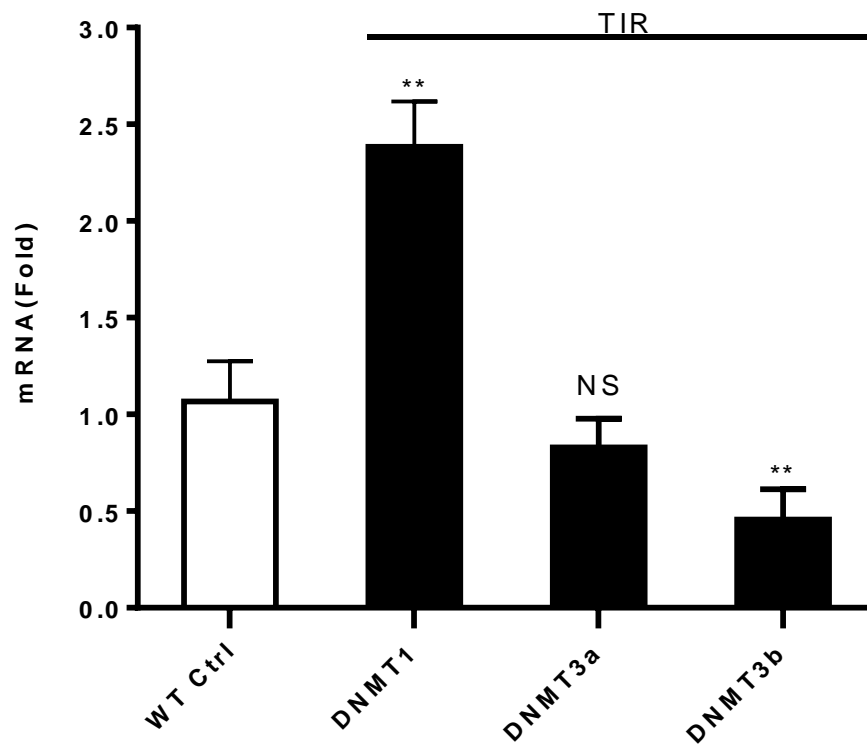
Fig 3.6. TIR is correlated with upregulation of DNMT1 expression. Five TIR clones with different sensitivities and one wild type (RAW 264.7 macrophage) clone were analyzed for DNMT1 mRNA levels using quantitative real time PCR analysis. Cell death levels were measured using MTT assay after treating cells with LeTx (LF 500ng/ml, PA 1μg/ml) for 5 hours. Correlation between cell death and DNMT1 expression was calculated using the Graphpad program (R^2= correlation coefficient). Data are expressed as means and SD (n=3).
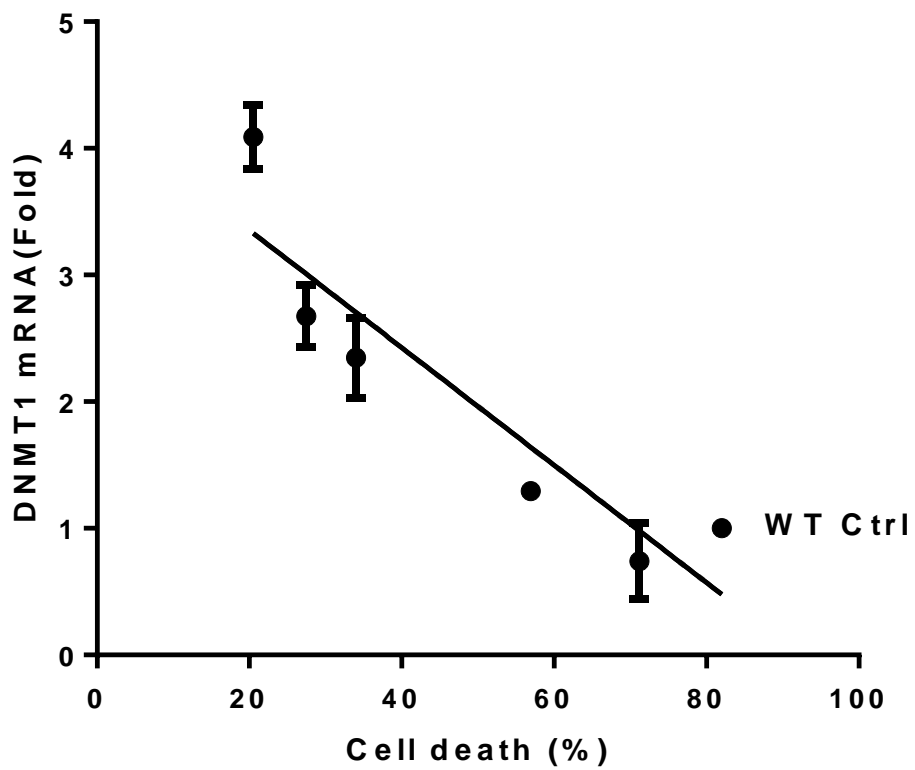
R^2 : 0.8459, Y = -0.04637*X + 4.281

Fig 3.7. Inhibition of DNMT1 sensitizes TIR cells to pyroptosis.

(A) Quantitative real time PCR analysis of siRNA knock down of DNMT1 in RAW 264.7 cell. TIR cells were transfected with scrambled or DNMT1 targeting (si-DNMT1) siRNAs for 48 hours. Treated cells were processed for total RNA purification and cDNA preparation to analyze knock down efficiency by quantitative RT-PCR. Data were normalized by the GAPDH expression levels in each sample. (B) TIR cells were transfected with scrambled or DNMT1 targeting siRNA (si-DNMT1) for 48 hours followed by treatment with LeTx (500ng/ml LF and 1µg/ml PA) for 5 hours. Cell death was then measured by MTT. (C) Wild type (RAW 264. 7 macrophage) were transfected with scrambled siRNAs or siDNMT1 for 48 hours and then treated with LeTx (100ng LF & 200ng PA) for 24 hours. Global methylation rates of surviving cells were then measured. Data are expressed as means and SD (n=3), * P≤ 0.05, **P≤0.01, and *** P≤0.005 (Student's t-test).

A)
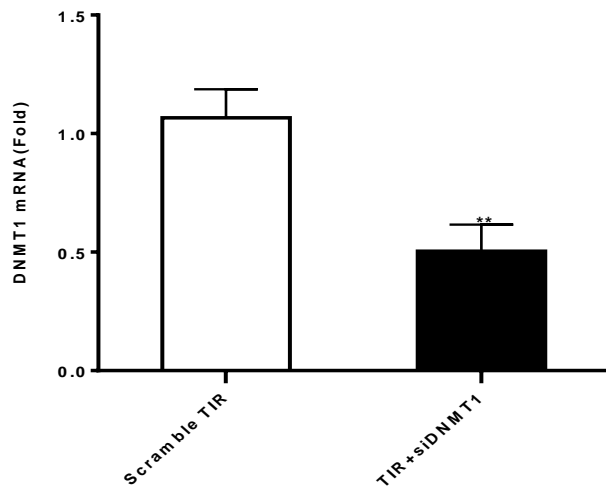
B)
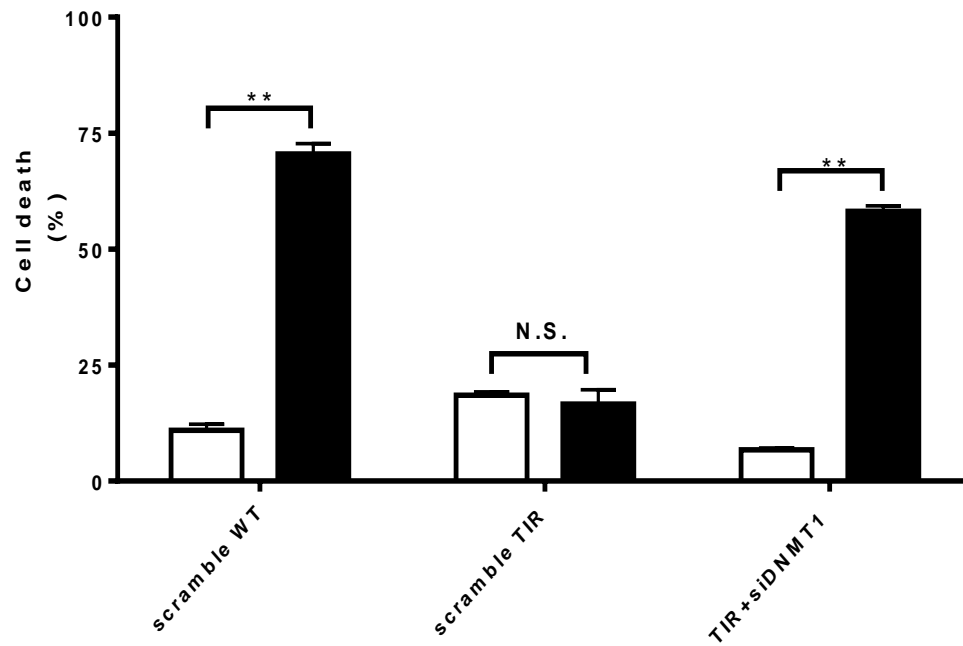
C)
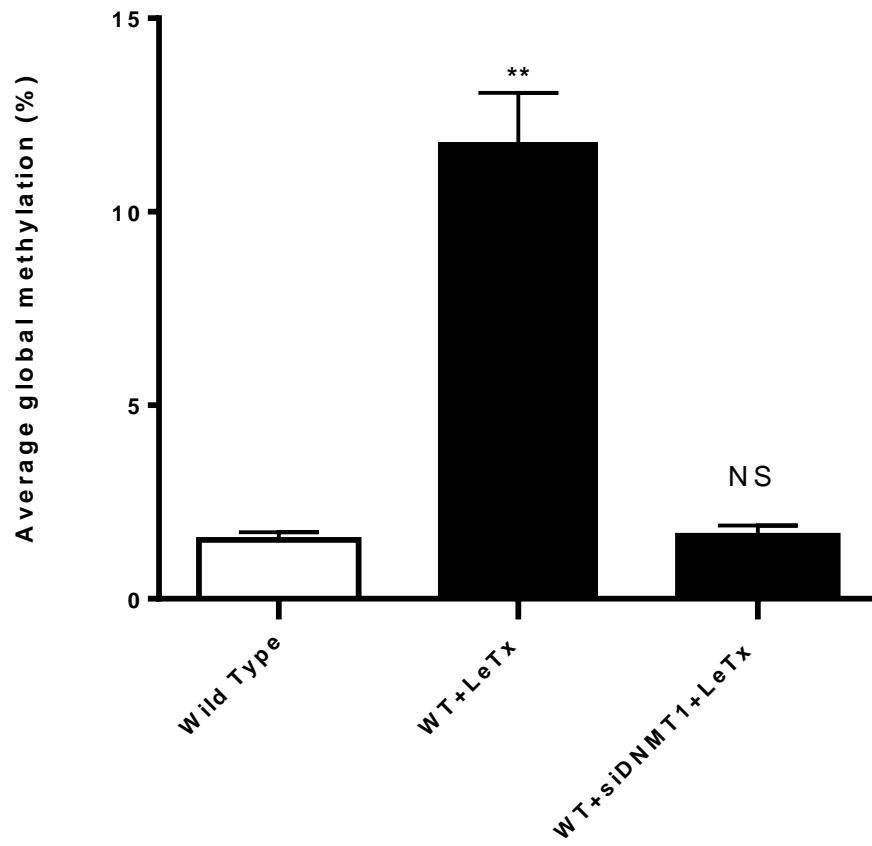
3.2.4. HDAC8 is involved in maintenance of TIR.

Following up the chemical inhibitor experiments (Fig 3.3), expression of various HDACs including HDAC1, 2, 5, 8, and 9 were analyzed using qPCR. Among them, HDAC8 and 9 were up-regulated more than 2 fold in TIR cells, whereas HDAC 1, 2, and 5 were down-regulated (Fig. 3.8). These results suggest that HDAC 1, 2 and 5 were not involved in TIR maintenance, which is consistent with the HDAC 1, 2 and 3 inhibitor mocetinostat results that showed no effects on TIR cells (Fig 3.3A). When multiple LeTx-sensitive and resistant clones were examined for HDAC8 expression levels, a strong correlation between expression of HDAC8 and TIR phenotypes ($R^2 =0.79$) was shown.

To further confirm the role of HDAC8 in TIR, HDAC 8 was knocked down with HDAC8-specific si-RNAs and examined for LeTx sensitivity. As expected, HDAC8-specific si-RNA down-regulated HDAC8 expression and TIR cells knocked down became sensitive to LeTx-induced pyroptosis but not in scrambled si-RNAs (Fig3.10A & B). Global methylation was measured using genomic DNA purified from HDAC8 specific knocked down wild type cells followed by LeTx treatment for 24 hours. Though LeTx treated wild type showed a 5 fold increase in global methylation level, HDAC8 knockdown did not show an increase in methylation, suggesting that HDAC8 also plays a role in global methylation induced by LeTx (Fig 3.10 C).

Fig 3.8. HDAC8 & HDAC9 are upregulated in TIR.

mRNAs from wild type (RAW 264.7 macrophage) and TIR cells were collected and analyzed for HDAC1, 2, 5, 8, and 9 by quantitative real-time PCR. Data are expressed as means and SD (n=3), * P≤ 0.05, **P≤0.01, and *** P≤0.005 (Student's t-test).
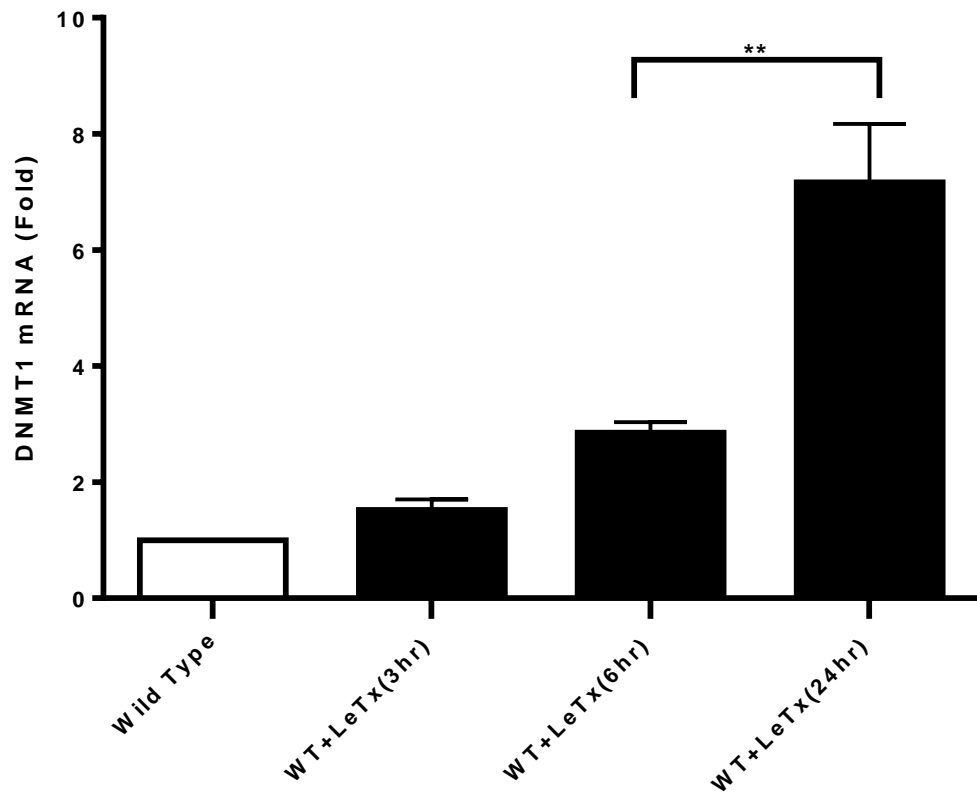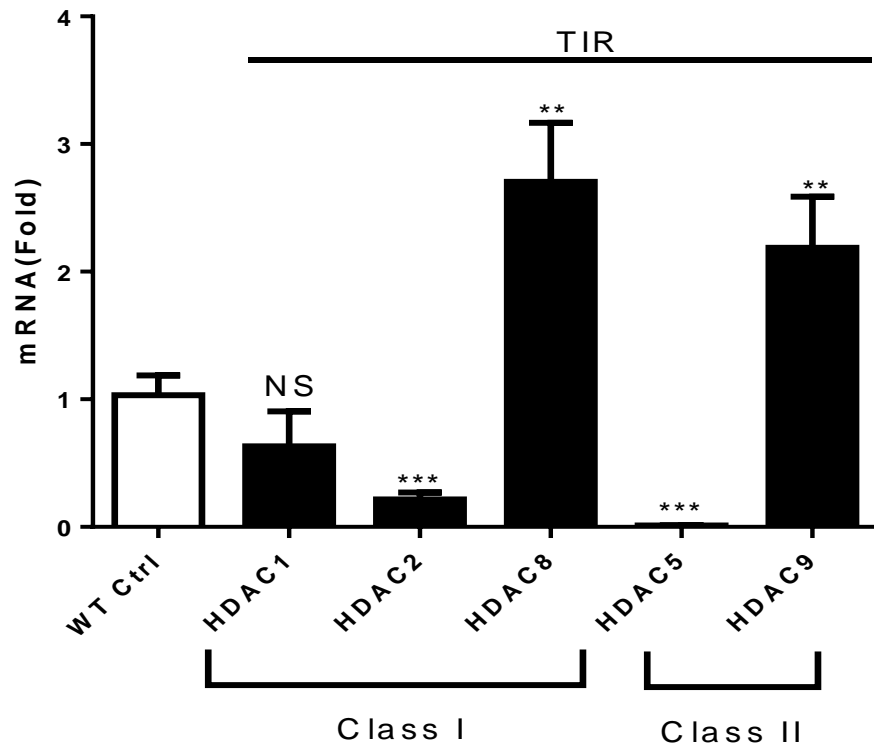
Fig 3.9. TIR is correlated with HDAC8 upregulation. Five TIR clones with different sensitivities and one wild type (RAW 264.7 macrophage) clone were analyzed for HDAC8 mRNA levels using quantitative real time PCR analysis. Cell death levels were measured using MTT assay after treating cells with LeTx (LF 500ng/ml, PA 1μg/ml) for 5 hours. Correlation between cell death and HDAC8 expression was calculated using the Graphpad program (R^2= correlation coefficient). Data are expressed as means and SD (n=3).
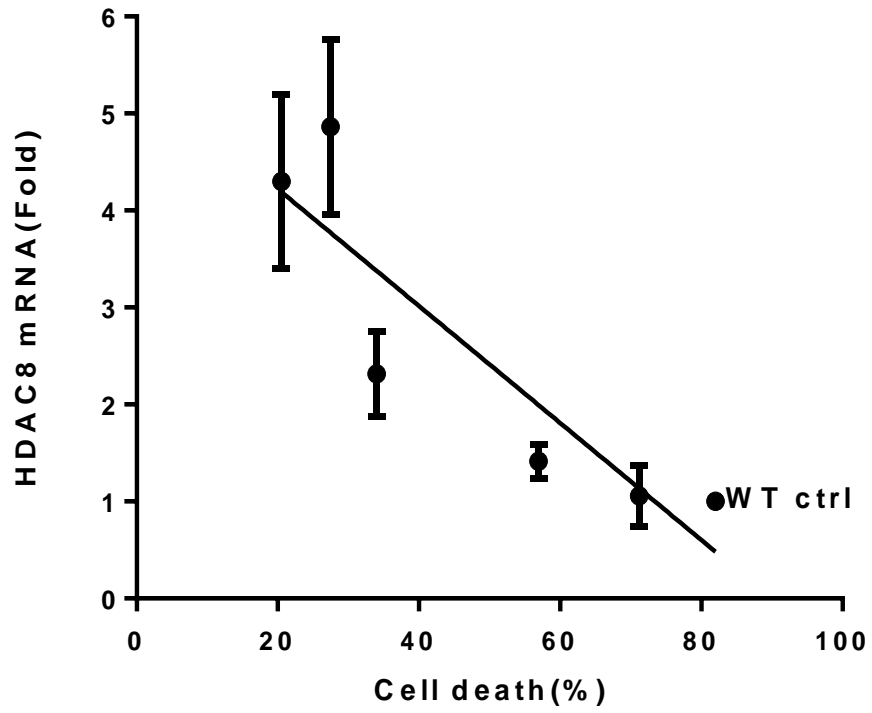
R^2: 0.7952, Y = -0.06030*X + 5.427

Fig 3.10. Inhibition of HDAC8 sensitizes TIR cells to pyroptosis.

(A) Quantitative real time PCR analysis of siRNA knock down of HDAC8 in RAW 264.7 cells. TIR cells were transfected with scrambled or HDAC8 targeting (si-HDAC8) siRNAs for 48 hours. Treated cells were processed for total RNA purification and cDNA preparation to analyze knock down efficiency by quantitative RT-PCR. Data were normalized by the GAPDH expression levels in each sample. (B) TIR cells were transfected with scrambled or HDAC8 targeting si-RNAs (si-HDAC8) for 48 hours, followed by treatment with LeTx (500ng/ml LF and 1μg/ml PA) for 5 hours. Cell death was then measured by MTT. (C) Wild type cells (RAW 264.7 macrophage) were transfected with scrambled siRNA or si-HDAC8 for 48 hours followed by treatment of LeTx (100ng LF & 200ng PA) for 24 hours. Global methylation rates were measured for each sample. Data are expressed as means and SD (n=3), * P≤ 0.05, **P≤0.01, and *** P≤0.005 (Student's t-test).

A)

B)

59
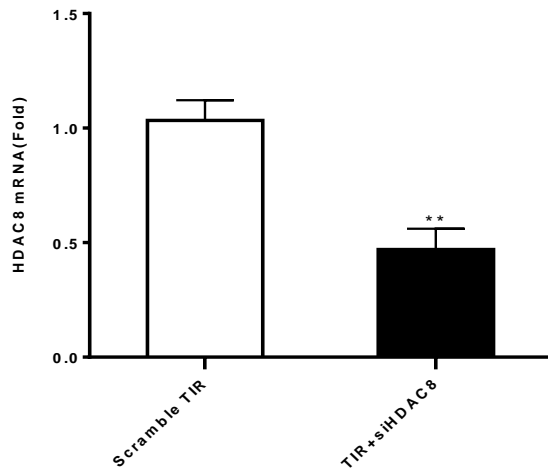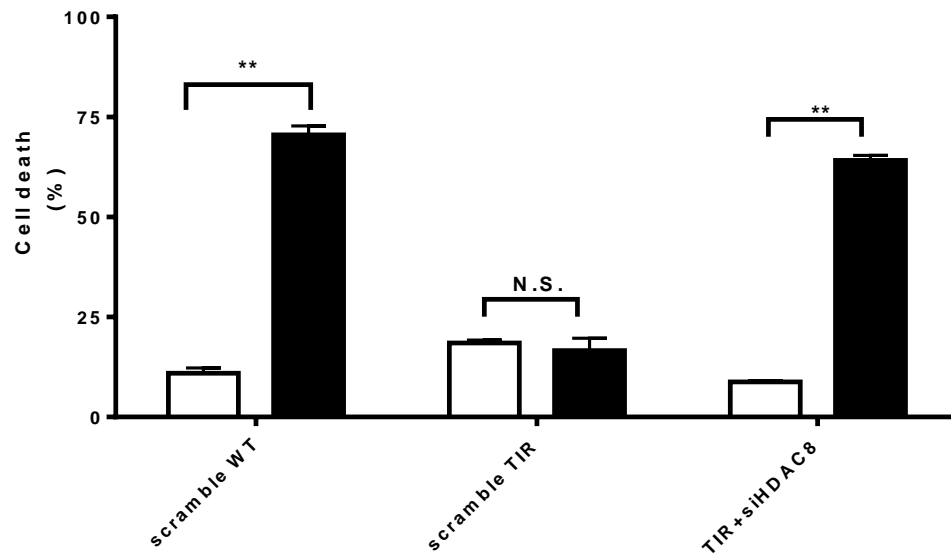
C)
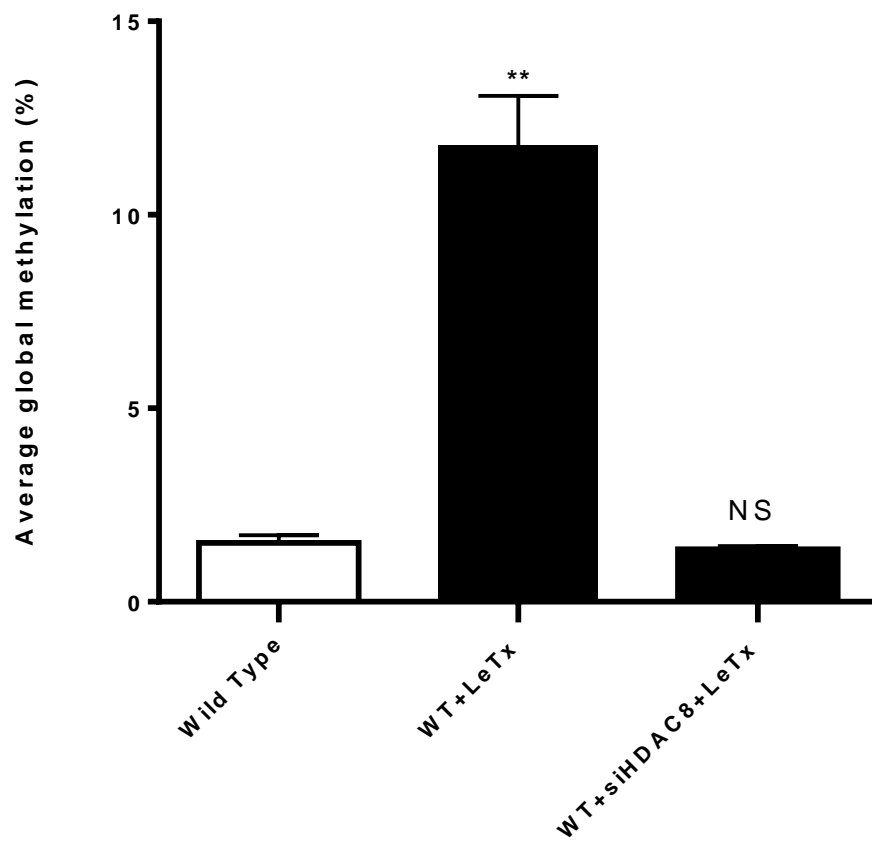
3.3. Down-regulation of BNIP3 & BNIP3L is mediated through DNMT1 and HDAC8.

3.3.1. DNMT1 is involved in the down regulation of BNIP3& BNIP3L in TIR cells.

We previously documented that TIR is in part mediated by down-regulation of BNIP3 and BNIP3L[50]. Indeed, TIR cells expressed BNIP3 and BNIP3L to 40% of the levels expressed in wild type cells (Fig 3.11). TIR cells treated with azacitidine (2.0μM Azacitidine for 24 hours) significantly up-regulated expression of both BNIP3 and BNIP3L at the mRNA levels up to 10- and 15-folds, respectively, (Fig 3.12). Similarly, knocking down DNMT1 by siDNMT1 up-regulated expression of BNIP3 (~8-fold) and BNIP3L (20-fold) in TIR cells (Fig 3.13), suggesting that methylation by DNMT1 is involved in down regulation of BNIP3 and BNIP3L.

3.3.2. Methylations in CpG Islands of BNIP3 & BNIP3L are not involved in TIR.

To examine whether TIR cells harbor higher levels of methylation in CpG islands of BNIP3 and BNIP3L, both conventional bisulfite sequencing and pyro-sequencing methods were used. Bisulfite treatment is most commonly used method to identify 5 methyl cytosine, m (5)-c, which is methylated cytosine by DNA methyltransferase. This experimental approach is based on the principle that methylation happened on the cytosine residue of dinucleotide CpG, and treatment of DNA with bisulfite deaminated cytosine, producing unmethylated cytosine residues to urasile, but left 5-methylcytosine residues unaffected as cytosine[100].This, by PCR, is converted to thymine. The final result is the creation of an artificial single nucleotide polymorphism (C, if methylated, and T if not methylated) that can be analyzed using several common sequencing techniques[101]. After bisulfite treatment, one of the CpG islands identified in the gene encoding BNIP3 was amplified and sequenced using a conventional cloning method as previously described in methods section (Section 2.8.1). Sequencing five of the clones from wild type and TIR cells showed no methylation in the CpG island of BNIP3 (Fig 3.14B). Pyroassay is a powerful sequencing method which detects nucleotide incorporation by proportional emission of light in each pyrosequencing cycle[102, 103]. For methylation analysis, biotin labeled, single stranded PCR products generated from bisulfite-treated DNA were used as a template with an internal primer[104]. Pryoassay can quantify

methylation frequencies in CpG islands and distinguish between methylated and unmethylated sequences. I prepared genomic DNA from wild type RAW 264.7 macrophage and TIR cells and Qiagen conducted bisulfite treatment followed by pyroassay. In line with the previous conventional bisulfite sequencing results, bisulfite pyroassay showed that 13 consecutive positions in longest CpG Islands of BNIP3 and BNIPL in wild-type and TIR cells were mostly unmethylated and no apparent differences were detected (Fig 3.15). However, the size for bisulfite sequencing for both conventional and pyroassay is limited up to 400 bp as upper limit due to DNA fragmentation which can occur during the bisulfite treatment[101]. In addition, the high redundancy of the target sequence due to the original GC richness creates long stretches of thymines, which are often difficult to read for the polymerases[105]. Hence, extensive regions of CpG islands in BNIP3 and BNIP3L which can be more than 1000 bp long are still to be sequenced.

Fig 3.11. Bnip3 and Bnip3L are down regulated in TIR. mRNA expressions of (A) BNIP3 and (B) BNIP3L were analyzed relative to GAPDH by using real time quantitative PCR in wild Type (RAW 264.7 cells) and TIR cells. Data are expressed as means and SD (n=3), * P≤ 0.05, **P≤0.01, and *** P≤0.005 (student's t-test).

A)
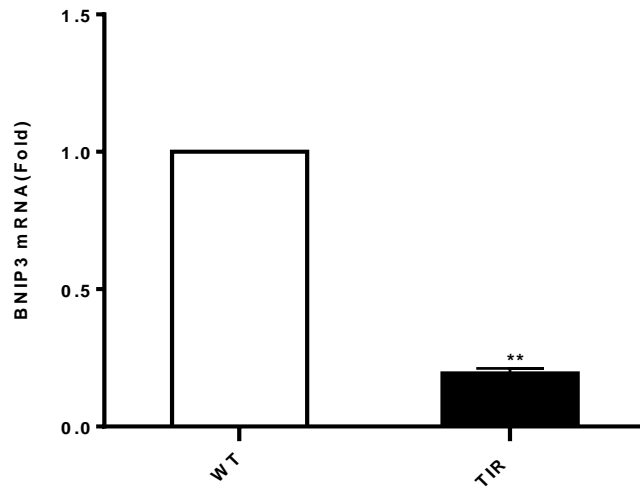
B)
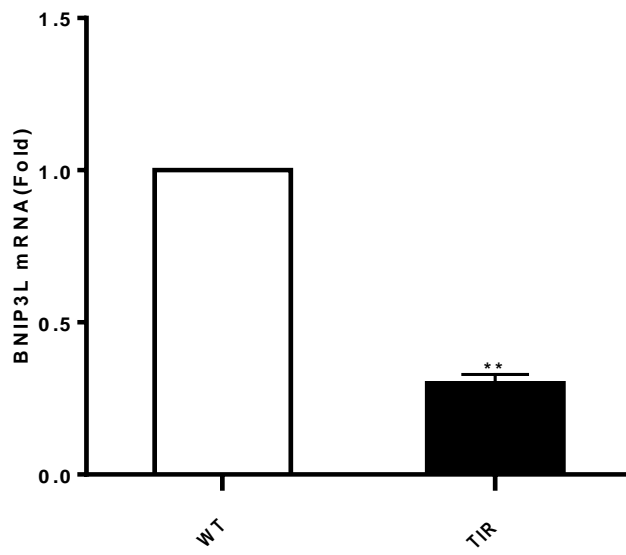
Fig 3.12. The DNA methyltransferase inhibitor azacitidine induces BNIP3 & BNIP3L expression in TIR cells. Wild Type (RAW 264.7 macrophage) and TIR cells were pretreated with 2.0μM azacitidine for 24 hours and mRNA levels of (A) BNIP3 and (B) BNIP3L relative to GAPDH were measured by real-time PCR. Data are expressed as means and SD (n=3), * P≤ 0.05, **P≤0.01, and *** P≤0.005 (Student's t-test).

A) BNIP3
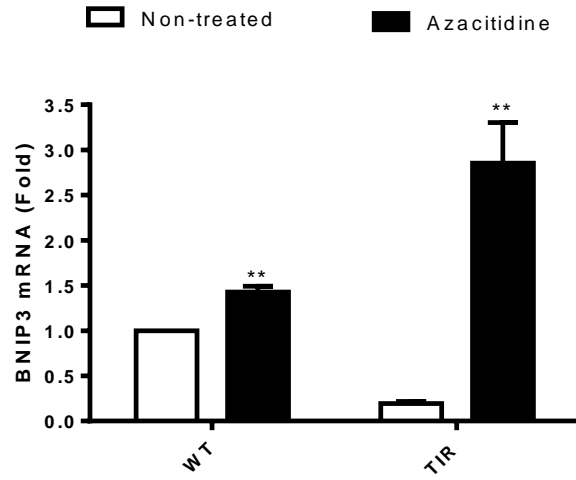
B) BNIP3L
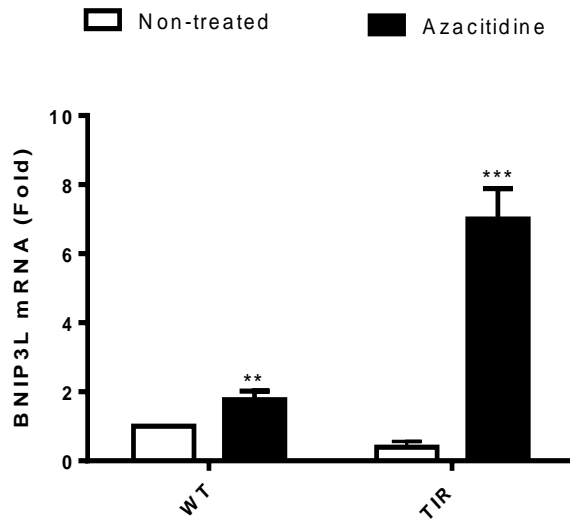
Fig 3.13. Knocking down DNMT1 by siRNA enhances BNIP3 and BNIP3L
expression in TIR cells.

(A) Quantitative real time PCR analysis of siRNA knock down of DNMT1 in RAW 264.7 cell. TIR cells were transfected with scrambled or DNMT1 targeting (si-DNMT1) siRNAs for 48hrs. Treated cells were processed for total RNA purification and cDNA preparation to analyze knock down efficiency by quantitative RT-PCR. Data were normalized by the GAPDH expression levels in each sample (B) TIR cells were transfected with scrambled siRNAs or DNMT1 targeting siRNAs (si-DNMT1) for 48 hours and expression of BNIP3 and BNIP3L were analyzed by real time quantitative PCR. Data are expressed as means and SD (n=3), * $P \leq 0.05$, **$P \leq 0.01$, and *** $P \leq 0.005$ (Student's t-test).

A)
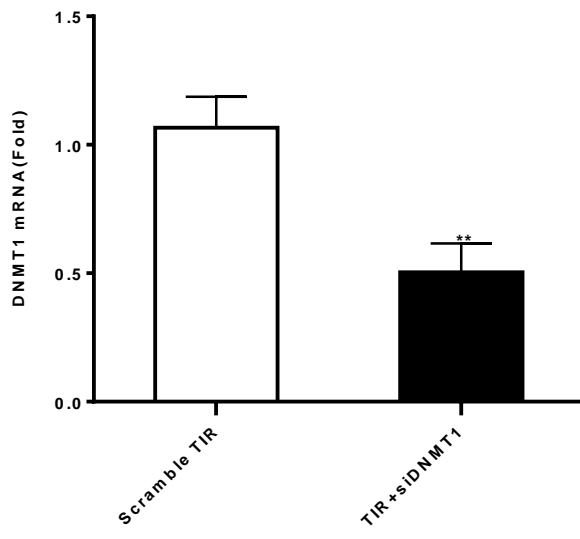
B)
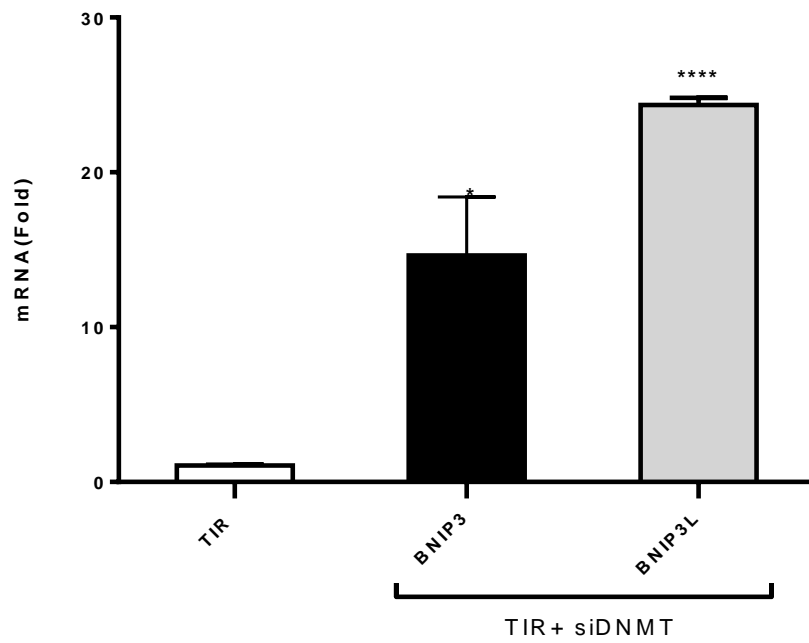
Fig 3.14. CpG islands of BNIP3 was not methylated.

(A) The CpG islands of BNIP3 were identified using epigenomic tools from NCBI[106]. (B) Genomic DNAs were purified from wild type and TIR cells and treated with bisulfite. PCR was conducted with the bisulfite specific primers and sequences of amplicons (125bp) were analyzed using bacterial cloning method as previously described in the method section (Section 2.8.1). Open and closed circles respectively represent unmethylated and methylated CpG dinucleotides (Black circle: methylated, White circle: unmethylated), respectively (N=5) (C) Sequence information of amplicon after untreated and treated bisulfite treatment for both wild type and TIR cells were identified.

A) CpG Islands of BNIP3
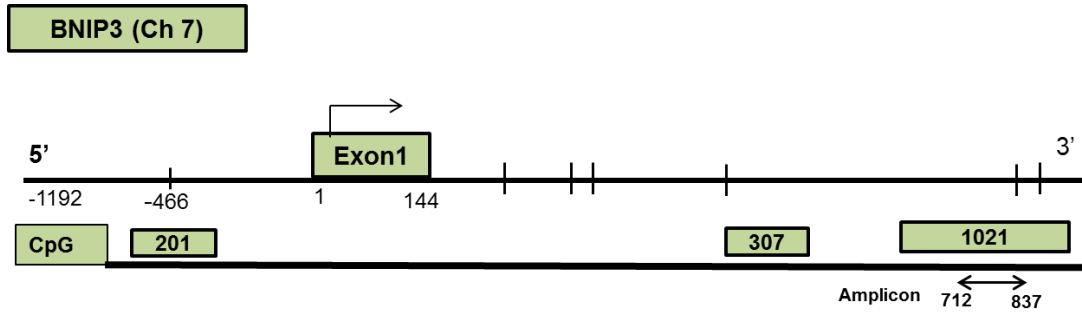
B)

Bisulfite sequencing of CpG Island of BNIP3 (125bp)
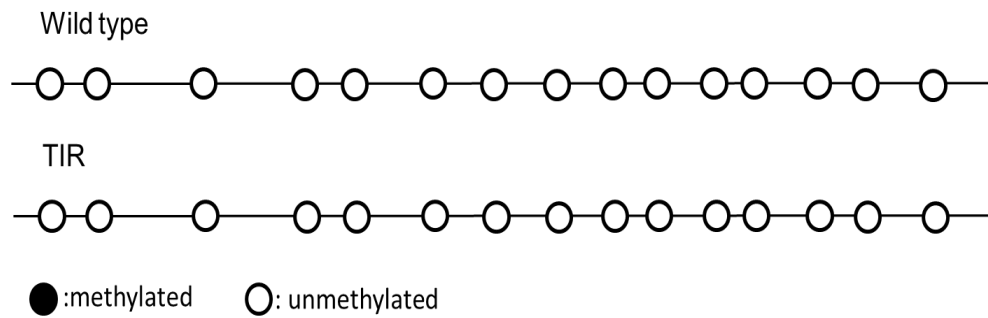
C)

Original sequence

TGAAGCCAGGCTGGAGGTGGGCAGACGTGGGCGGGCTCCGAGATAGGCGTGGCATGAGGACGT
GCGGCCAGGTTTTTGGGCGTCTGGCCTTGGGTGCTGAGTTTGCCCCTCCTGCTGTTAATCACTAG

Modified cytosine after bisulfite treatment in BNIP3

Wild Type

TGAAGTTAGGTTGGAGGTGGGTAGATGTGGGTGGGTTTTGAGATAGGTGTGGTATGAGGATGT
GTGGTTAGGTTTTTGGGTGTTTGGTTTTGGGTGTTGAGTTTGTTTTTTTTGTTAATCACTAG

TIR

TGAAGTTAGGTTGGAGGTGGGTAGATGTGGGTGGGTTTTGAGATAGGTGTGGTATGAGGATGT
GTGGTTAGGTTTTTGGGTGTTTGGTTTTGGGTGTTGAGTTTGTTTTTTTTGTTAATCACTAG

71

Fig 3.15. Pyroassay analysis of methylated BNIP3 & BNIP3L

Bisulfite pyroassay was conducted to analyze methylation status of 13 consecutive positions in CpG islands of (A) BNIP3 & (B) BNIP3L. (C) Methylation levels were calculated using Pyro Q-CpG software. The assays were performed by Qiagen (Maryland, USA).

A)
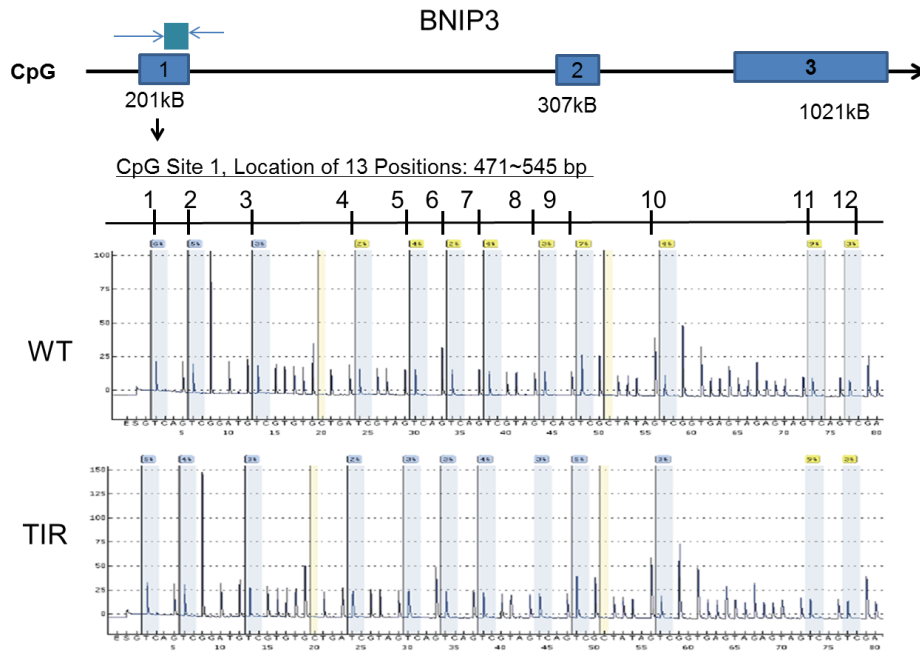
B)
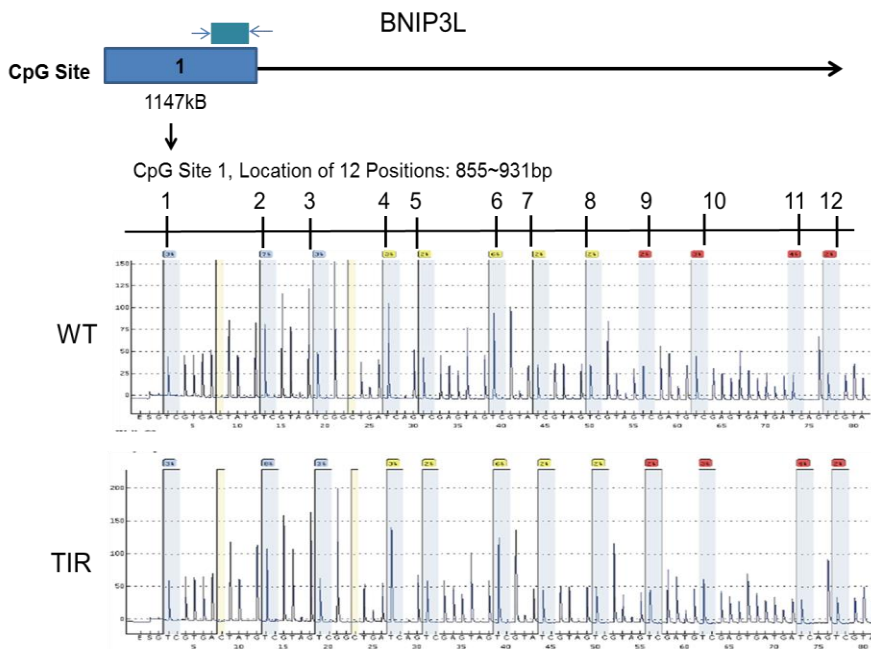
C)

Table 3.1. Bisulfite pyroassay results of BNIP3 & BNIP3L

Gene	Type	Metyhlation (%)											
		Position No.											
		1	2	3	4	5	6	7	8	9	10	11	12
BNIP3	WT	5.84	4.92	3.19	1.96	3.92	2.45	3.67	2.65	6.94	3.57	9.32	2.53
	TIR	5.35	4.25	2.70	2.43	2.95	3.41	4.35	2.79	5.43	2.90	9.27	2.56
BNIP3L	WT	2.79	7.42	2.98	3.27	2.15	6.16	2.4	2.18	2.22	3.12	3.93	1.96
	TIR	2.97	7.67	3.27	2.93	2.04	6.37	1.98	2.32	2.03	3.31	4.26	1.67
Positive Ctrl	WT	3.11	8.13	3.07	3.73	1.53	4.33	2.58	2.20	1.99	3.49	4.52	1.54
	Meth*	98.4	100	91.2	99.4	86.5	100	89.3	84.6	85.2	100	97.5	NA

*: Methylated positive control

3.3.3. HDAC8 is involved in the down-regulation of BNIP3 & BNIP3L in TIR cells.

HDAC8 expression was increased in TIR cells (Fig 3.8) and knocking it down by siRNAs sensitized TIR cells to LeTx-induced pyroptosis (Fig 3.10). Therefore, I examined whether knocking down HDAC8 enhanced BNIP3 and BNIP3L expression in TIR cells. As expected, TIR cells treated with HDAC8 targeting siRNAs induced a 14 fold and 30-fold higher expression of BNIP3 and BNIP3L, respectively, than those of non-treated TIR cells (Fig 3.16). Collectively, together with the previous DNMT1 knocking down (Fig 3.11), down-regulation of BNIP3 and BNIP3L in TIR cells was likely mediated through epigenetic mechanisms involved in both DNA methylation and histone deacetylation.

3.3.4. Deacetylation at histone 3 lysine 27 (H3K27) is involved in down regulation of BNIP3 & BNIP3L expression.

Since HDAC8 was shown to be involved in TIR and suppression of BNIP3 and BNIP3L, histone acetylation could have been involved in TIR maintenance. To find targets of HDAC8 responsible for BNIP3 and BNIP3L expression, acetylated histones binding to BNIP3 and BNIP3L encoding gene were searched through the genome-wide epigenetic marker database[107] (ENCODE) and we found that histone H3 acetylated at lysine 27 (H3K27Ac) was shown to be commonly involved in expression of both BNIP3 and BNIP3L[107](Fig 3.17). Indeed, Western blot analysis using H3K27Ac-specific antibodies showed 5-fold higher levels of overall H3K27Ac immunoreactivity in wild type than TIR cell extracts (Fig 3.18). Also, treatments of panobinostat (100nM) showed a 9 fold increase and treatment of azacitidine (2.0μM) showed a 12 fold increase in H3K27Ac levels compared to non-treated TIR (Fig 3.18). These results collectively suggest that TIR cells suppress BNIP3 and BNIP3L through deacetylating and methylatng H3K27, which at least in part renders resistance to LeTx-induced pyroptosis in TIR cells. In addition, ChIP (Chromatin Immunoprecipitation) assay showed that H3K27Ac was enriched in wild type whereas it is down regulated in TIR for BNIP3 expression, suggesting that H3K27Ac functions as an enhancer for the expression of BNIP3 (Fig 3.19A) through histone modification. However, enrichment of H3K27Ac in wild type did not show significant difference compared to TIR for BNIP3L expression (Fig 3.19B), suggesting

that other enhancers such as H3K9Ac or H3K36Ac or histone methylation of H3K4Me3 are involved to regulate expression of BNIP3L.

Fig 3.16. Knocking down HDAC8 by siRNAs enhances BNIP3 & BNIP3L expression in TIR cells.

(A) Quantitative real time PCR analysis of siRNA knock down of HDAC8 in RAW 264.7 cell. TIR cells were transfected with scrambled or HDAC8 targeting (si-HDAC8) siRNAs for 48 hours. Treated cells were processed for total RNA purification and cDNA preparation to analyze knock down efficiency by quantitative RT-PCR. Data were normalized by the GAPDH expression levels in each sample (B) TIR cells were transfected with scrambled siRNAs or HDAC8 targeting siRNAs (si-HDAC8) for 48hrs and expression of BNIP3 and BNIP3L were analyzed by real time quantitative PCR. Data are expressed as means and SD (n=3), * P≤ 0.05, **P≤0.01, and *** P≤0.005 (Student's t-test).

A)
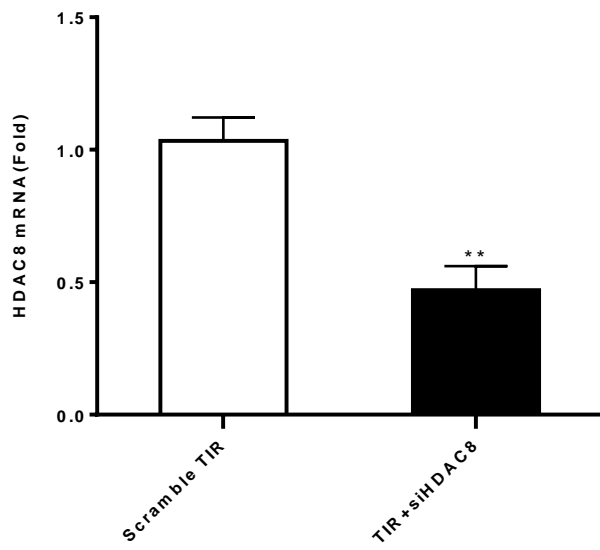
B)
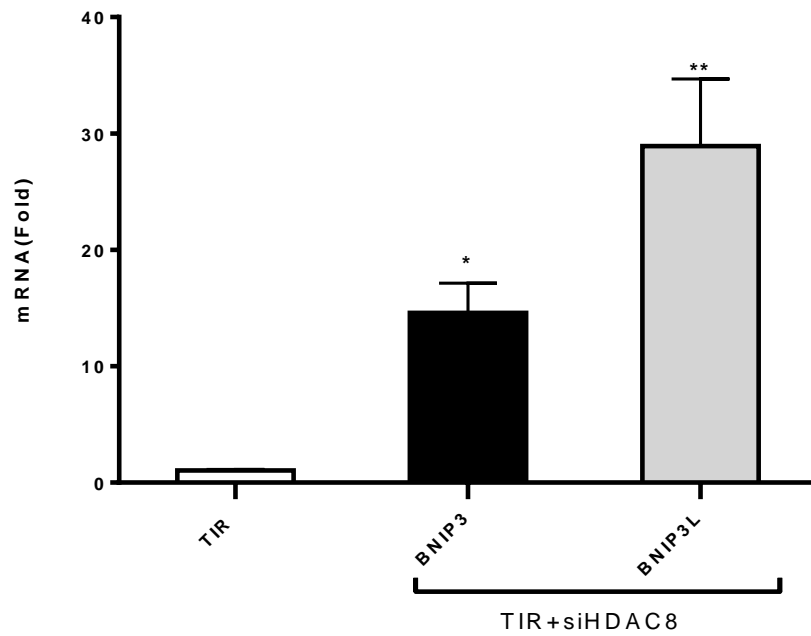
Fig 3.17. Histone modification profiles of H3K27Ac which interact with BNIP3 and BNIP3L. Histone modification site search using ENCODE[107, 108], the signal of H3K27Ac targeting (A) BNIP3 and (B) BNIP3L where histone modification occur were identified in the promoter region (Arrow → indicates primer design site for ChIP assay). Snap shot of from UCSC genome browser was taken showing for GC %, CpG islands, Chip-Seq for histone modification for the bone marrow derived macrophage cell line (BMDM).

A)

BNIP3

B)
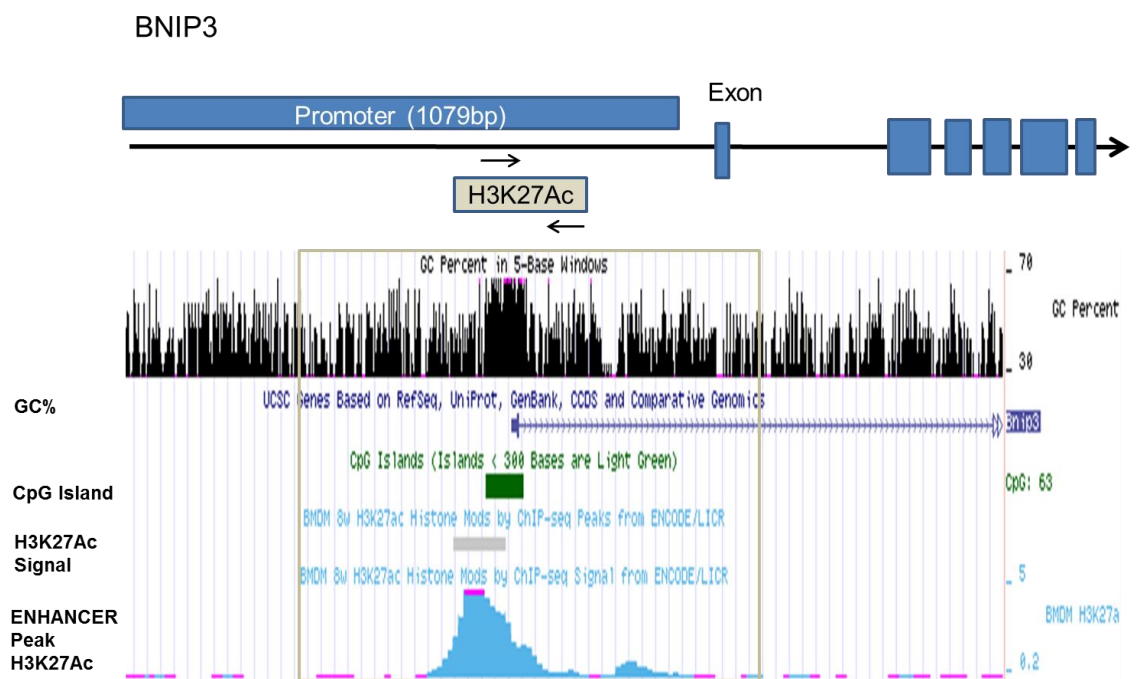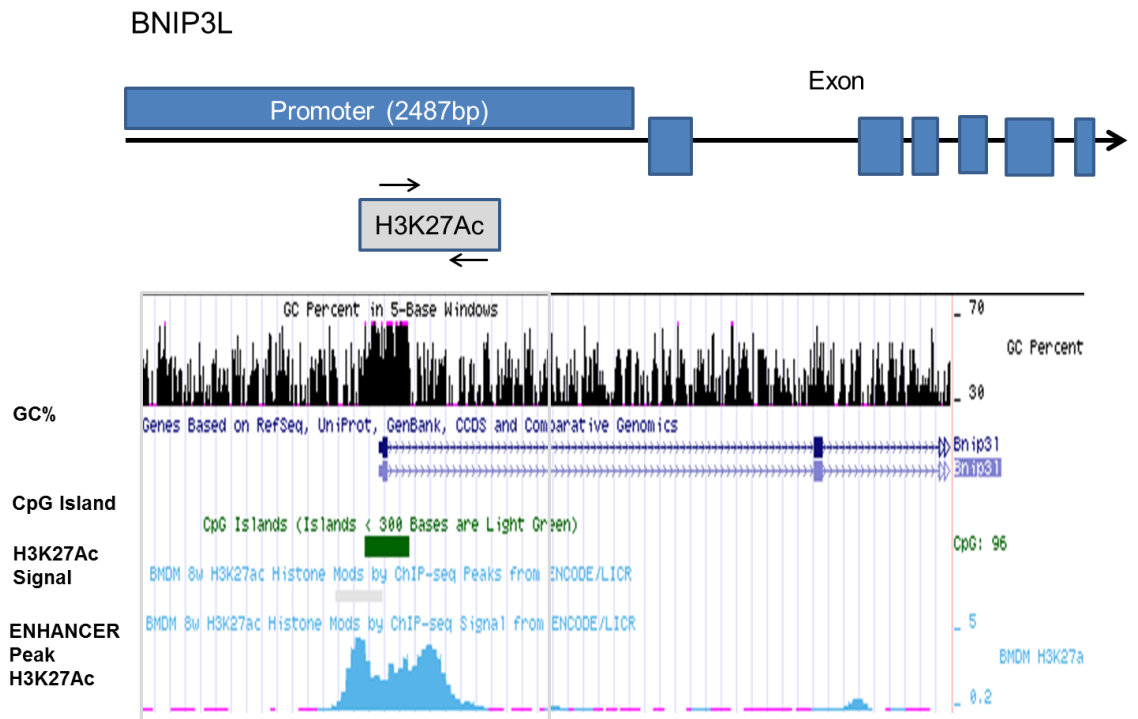
BNIP3L

Fig 3.18. Histone modification site for down regulation of BNIP3 gene expression in TIR (A) Expression of H3K27Ac in wild type (RAW 264.7 macrophage) and TIR were analyzed using immunoblots. β-actin was used as loading controls. (B) TIR cells were pretreated with histone deacetylase inhibitor (100 nM Panobinostat: PN) or DNA methyltransferase (2.0 μM Azacitidine: Aza) inhibitor and levels of H3K27 acetylation in wild type and TIR were analyzed using immunoblots. Immunoreactivity of H3K27Ac was analyzed using NIH image program. Data are representative of three independent experiments. Data are expressed as means and SD (n=3), * P≤ 0.05, **P≤0.01, and *** P≤0.005 (Student's t-test).

A)
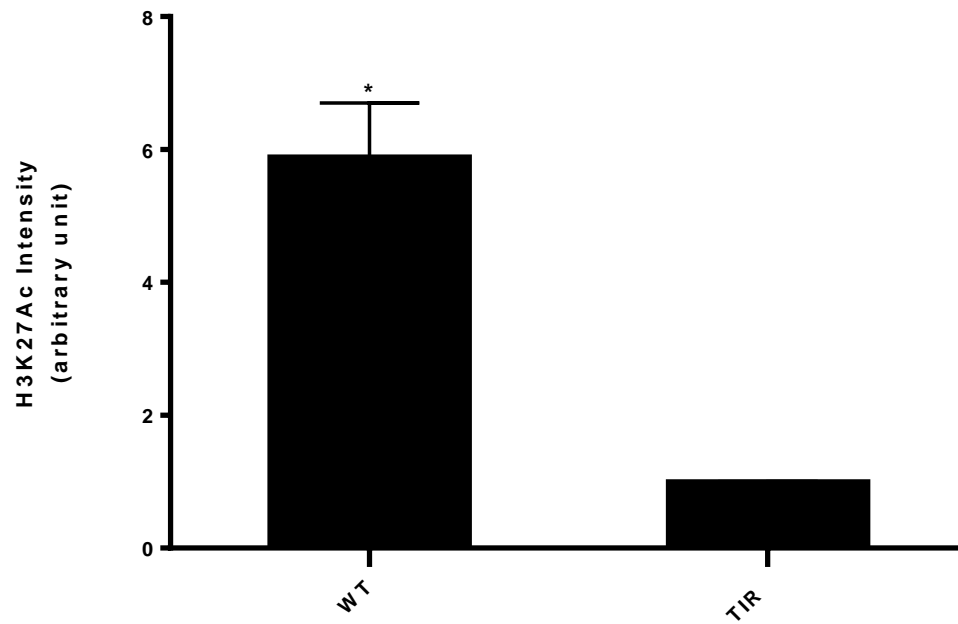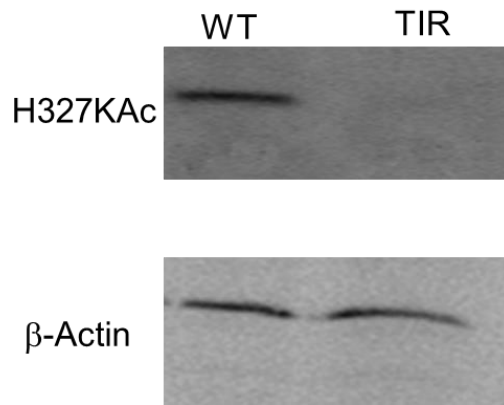
B)
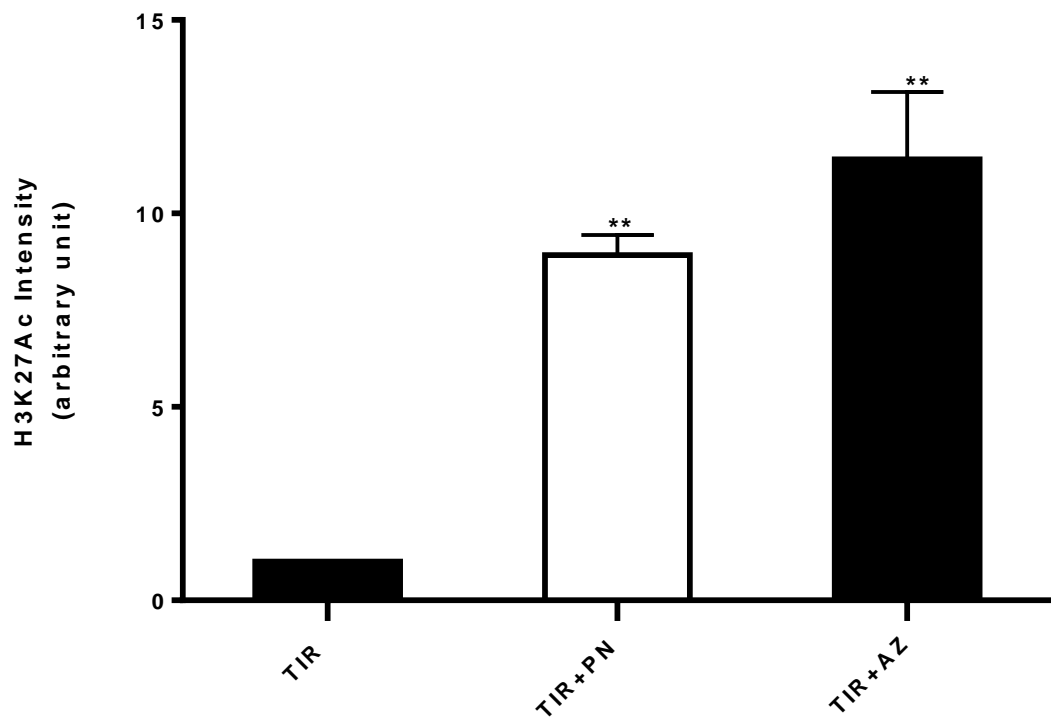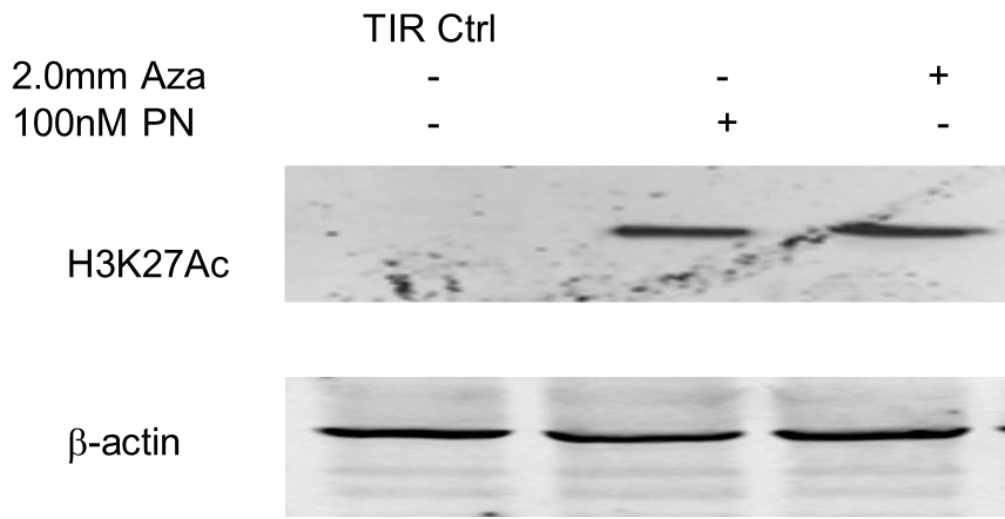
Fig 3.19. H3K27Ac binding to the promoter regions of BNIP3 is suppressed in TIR.

Promoter binding of the BNIP3 and BNIP3 to H3K27Ac was evaluated by Chromatin Immunoprecipitation (ChIP) analysis. Genomic DNAs from wild type (RAW 264.7 macrophages) and TIR cells were prepared, sonicated, and, immunoprecipitated using antibodies against H3K27Ac, and control IgG. Immunoprecipitated DNAs were analyzed by quantitative real-time PCR using primers for (A) BNIP3 and (B) BNIP3L. For ChIP efficiency, % of input DNA recovered by immunoprecipitation, was determined by quantitative real-time PCR. Rabbit IgG serum was used as a background control.

(A) BNIP3 promoter
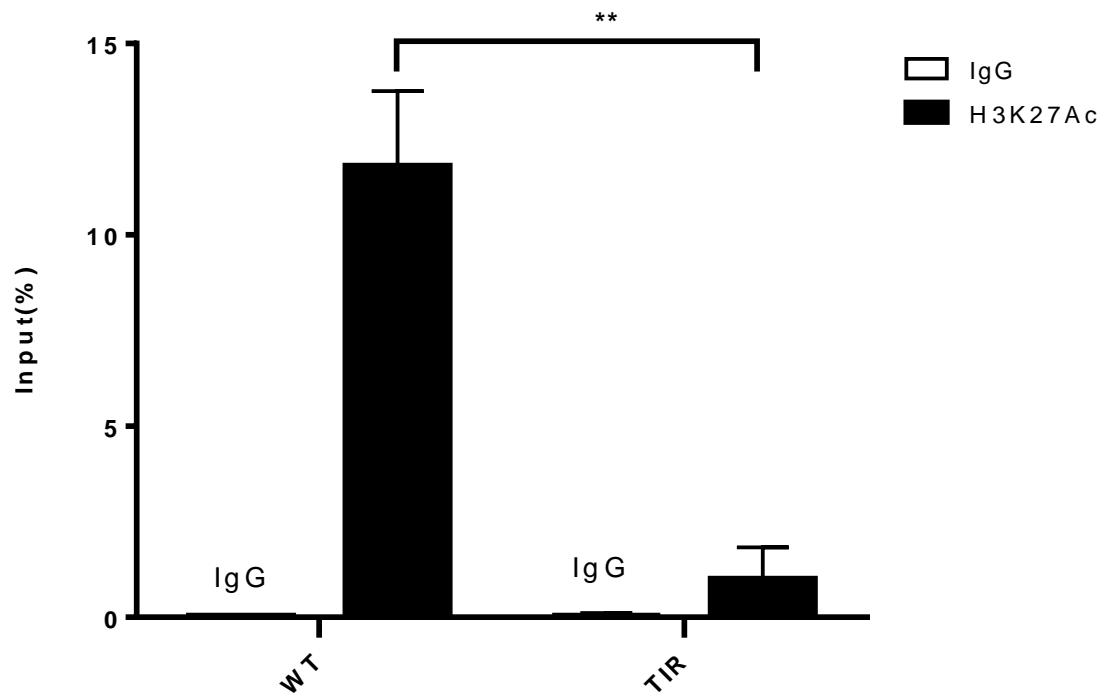
(B) BNIP3L promoter
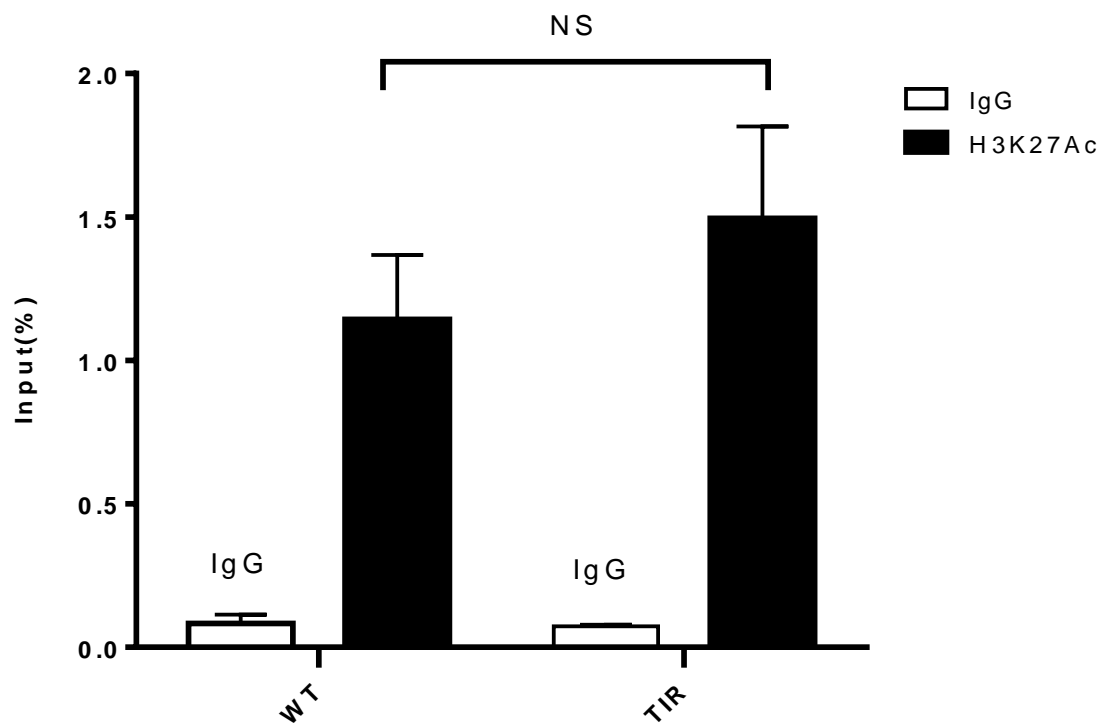
CHAPTER 4 - DISCUSSION

Epigenetic reprogramming is a cellular mechanism of gene regulation persisting throughout cell division. Here, I showed that toxin induced resistance (TIR) was an epigenetic adaptation of macrophages to LeTx-induced pyroptosis. Previously, several mechanisms of TIR were suggested. Salles et al. reported an adaptive ERK activation by a MEK-independent process or a general decrease in proteasome activity was known to be partially involved[69]. We previously have found that BNIP3 and BNIP3L were down regulated in TIR[50], conferring resistance to pyroptosis. Further, TIR cells were resistant to NLRP-1 inflammasome induced mitochondrial dysfunction, including mitochondrial inner membrane hyperpolarization, generation of reactive oxygen species (ROS), and depletion of the anti-oxidants[55]. However, specific mechanism how BNIP3 and BNIP3L were down regulated in TIR cells is still elusive and the mechanism needs to be further explored. In this study, we reported that DNMT1 and HDAC8 were required for maintaining TIR and it suppresses BNIP3 and BNIP3L in TIR. Also, H3K27Ac was decreased in TIR cells and it subsequently suppresses BNIP3. A previous study showed that LeTx inhibits histone H3 phosphorylation on serine 10 (H3S10) and suppresses IL-8 production[109]. It was speculated that the cleavage of MEKs by LeTx, resulting in their inactivation, is responsible for the lack of H3S10 phosphorylation, since the phosphorylation is mediated by the mitogen and stress-activated kinase (MSK) which is activated by p38 and ERKs. However, since TIR cells were normal in basal p38 and ERK activities (Fig 3.2), H3S10 phosphorylation is expected to be normal in TIR cells. This study detected a significant and rapid increase of global DNA methylations by LeTx treatments (Fig 3.4A), which was prevented by the DNMT inhibitor azacitidine and siRNAs targeting DNMT1 (Fig 3.4B &D). These results suggest that up-regulation of DNMT1 was responsible for at least in part of global DNA methylation induced by LeTx. Global DNA methylation was also detected in macrophages harboring non-functional NLRP1b (Fig 3.4D), suggesting that activation of NLRP1b was not involved in the changes. Other studies have also shown that LeTx inhibits phosphatidylinositol 3-kinase (PI3K) and protein kinase B (Akt) signaling cascades[110]. As mentioned earlier, high global DNA methylation by LeTx was not maintained in TIR cells (Fig 3.4C) and thus global DNA methylation *per se* was not likely involved in TIR. Interestingly, TIR cells

expressed a higher level of DNMT1 than those of wild type and the extent of LeTx-induced pyroptosis was negatively correlated with the levels of DNMT1 expression (Fig 3.6). These results suggest that DNA methylation at specific genome sites through DNMT1 was required for TIR maintenance; however, the identities of the genes are unknown.

Since DNMT1 was required for TIR, I further examined whether BNIP3/BNIP3L expression in TIR cells could be restored by the DNMT chemical inhibitor azacitidine and siRNAs targeting DNMT1. Indeed, suppression of BNIP3 and BNIL3L expression in TIR cells required at least in part DNMT1-mediated DNA methylation (Fig 3.3 & 3.7). However, DNA methylations in the promoter regions encoding BNIP3 and BNIP3L were not different between wild type and TIR cells (Fig 3.14). Considering the limits of this study in the number of bisulfite sequence analysis performed using the conventional cloning method (Fig 3.14B) and partial sequence by the pyroassay (Fig 3.15). In addition, suppression of BNIP3/BNIP3L by DNMT1 could have been mediated through suppression of other genes that positively regulate BNIP3/BNIP3L expression.

In addition to DNMT1, experiments with chemical inhibitors for enzymes involved in epigenetic reprogramming indicated that HDACs were required for maintaining TIR (Fig. 3.3). Also the broad spectrum HDAC inhibitor panobionostat, but not HDAC1,2 and 3-specific mocentinostat, rendered TIR cells sensitive to LeTx-induced pyroptosis (Fig.3.3), indicating that HDACs other than HDAC1,2, and 3 were required for TIR, Furthermore, qPCR analysis showed that HDAC8 and HDAC9, but not HDAC1, 2 and 5, were up-regulated in TIR cells. TIR cells became sensitized to LeTx-induced pyroptosis when HDAC8 was specifically knocked down by siRNAs. Collectively, these results suggested that HDAC8 was involved in the resistance mechanism of TIR cells. HDAC8 is a member of the class I histone deacetylase family. It forms transcriptional repressor complexes by associating with many different proteins (including pRb-E2F and mSin3A), and plays an important role in transcriptional regulation, cell cycle progression, and developmental events. HDAC8 also may play a role in smooth muscle cell contractility[111]. Gao *et al*. reported that knockdown of HDAC8 resulted in the increased expression of JAK2/STAT signaling leading to cytokine signaling in K562 and HEL cells[112].

Histone modification by HDAC and histone methylases can suppress BNIP3/BNIP3L expression. Given that DNA methylations in the promoter regions of BNIP3 and BNIP3L were not involved, histone acetylation levels could have contributed to their gene expressions in TIR cells. Several studies have elucidated that BNIP3 expression is regulated by epigenetic mechanisms such as DNA methylation and histone deacetylation and how transcription factor, Hypoxia Inducible Factor (HIF-1) influences expression of BNIP3 under hypoxic conditions[68, 92, 113-115]. For example, Murai *et al*. showed that BNIP3 expression was suppressed in hematopoietic tumors and it could be restored by the treatments of methyltransferase inhibitor, azacitidine[68], leading to hypoxia-mediated cell death. When they measured the acetylation of histone H3 in the 5' region of the gene using ChIP assays, gene expression was correlated with acetylation and inversely correlated with DNA methylation, suggesting that DNA methylation in the 5' CpG islands and histone H3 deacetylation responsible for silencing BNIP3 expression[68]. Previously, several studies demonstrated that DNMT1 and HDACs co-operatively work and induce gene silencing[94]. For example, Jones *et al*. suggested that methylated DNA assembled into chromatin and it binds to the transcription repressor MeCP2 as a methylation-specific transcriptional repressor, which recruits Sin3 histone deacetylase complex[94].

By using HDAC inhibitors in vitro system, several effects on the expression of many genes have been shown, resulting in cell differentiation, inhibition of proliferation and induction of apoptosis[92, 112, 115]. Underlying mechanism of HDAC inhibitors affecting on gene expression is described as acetylation, resulting in increased recruitment of transcription factors, which result is increased in expression of particular genes. However, HDACs can render gene suppression through targeting non-histones. For example, Zhou et al. showed that inhibition of HDAC1 increased ubiquitin-dependent proteasomal degradation of DNMT1, suggesting that HDACs is directly involved in regulation of DNMT1 stability[116]. Further Du et al. suggested that DNMT1 was destabilized by acetylation driven ubiquitination, through targeting DNMT1 for proteasomal degradation. On the other hand, HDAC1 and deubiquitinases such as HAUSP (Herpes virus associated ubiquitin specific protease) stabilized DNMT1[117].

Since HDAC8 was shown to be required for TIR, I further examined how histone deacetylation could influence BNIP3 and BNIP3L expression. Based on the ENCODE genome-wide epigenetic reprograming data base search[107], H3K27Ac was identified as a common enhancer for both BNIP3 and BNIP3L expression (Fig 3.17). Through Western blots and chromatin immunoprecipitation assay (ChIP), I examined whether H3K27Ac was decreased in TIR cells. As expected, the levels of H3K27Ac were substantially diminished in TIR cells, and TIR cells exposed to the HDAC inhibitor panobinostat or DNMT inhibitor azacitidine restored H3K27Ac levels (Fig 3.18). ChIP assays using H3K27Ac specific antibodies showed that H3K27Ac strongly interacted with the promoter regions of BNIP3 but not BNIP3L in wild-type cells, which was significantly diminished in TIR cells (Fig 3.19A). These results suggest that H3K27Ac is possibly deacetylated by HDAC8, and resulted in the suppression of BNIP3 expression in TIR cells. Unlike BNIP3, occupancy of H3K27Ac of the BNIP3L promoter was about 10 fold less in both wild type and TIR than those of BNIP3 (Fig 3.19B), suggesting that H3K27Ac did not sufficiently present in the promoter region of BNIP3L (Fig 3.19B). I speculate that histone acetylation of H3K27 in BNIP3L promoter region less frequently occurs and histone deacetylase will not be recruited to down regulate expression of BNIP3L. Though, H3K27Ac minimally contributed expression of BNIP3L, other histone modifications such as histone methylation and acetylation of other regions such as H3K9Ac or H3K36Ac may be involved. The ENCODE genome-wide epigenetic reprograming data base search also identified H3K9Ac and H3K36Ac as histone modification marker for BNIP3 and BNIP3L gene expression in leukemia cell line, respectively[107]. It has been previously reported that acetylation of H3K36 and H3K9 leads to activation of gene transcription as enhancer[118, 119]. It also has been shown that histone methylation enhances gene transcription; it is possible that mono methylation of H3K4 and H3K9, and tri methylation of H3K4 in BNIP3L activate gene transcription[120]. Examining the role of these acetylation sites of H3 in BNIP3 and BNIP3L expression will need to be further explored and it will provide insights into the mechanism of HDAC8 in TIR.

In summary, TIR cells induced high levels of DNMT1 and HDAC8 expression, which was responsible for maintaining TIR and suppressing expression of the cell death genes

BNIP3 and BNIP3L (Fig 4.1), conferring resistance in TIR cells. Although the mechanism of DNMT1 in TIR was undetermined, HDAC8 could have suppressed the expression of BNIP3 through deacetylating histones such as H3K27Ac. This study for the first time elucidates epigenetic mechanisms of TIR cells in macrophage.

Fig 4.1. BNIP3 and BNIP3L are down regulated through epigenetic mechanism mediated *via* DNMT1 and HDAC8. LeTx induces methylation in RAW 264. 7 macrophage cells and TIR and BNIP3 and BNIP3L partially methylated in TIR. LeTx subsequently recruits HDAC8, leading to down regulation of BNIP3 and BNIP3L. (Blue indicates unmethylated DNA and red indicates methylated DNA.)

Active transcription
(BNIP3/BNIP3L)

DNMT1
methylation
induced by LeTx

Unmethylated BNIP3/BNIP3L

HAT?

Methylated BNIP3/BNIP3L

Condensed chromatin site H3K27

Maintenance
of methylation
by DNMT1 &

HDAC8

Downregulation of
BNIP3 & BNIP3L

Recruitment of HDAC8 to methylated BNIP3 & BNIP3L

TIR
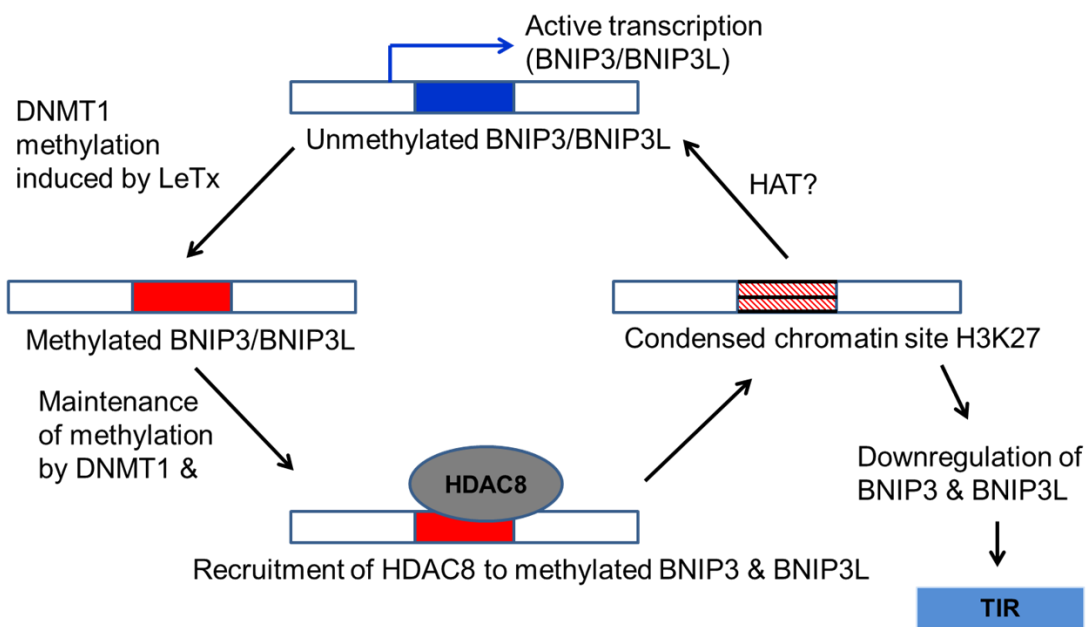
4.1. Further study

This study provided valuable information on the role of epigenetic reprograming in TIR. However, multiple limitations were also identified in this study. To further elucidate the mechanisms of TIR, the following experiments are suggested:

4.1.1. Validation of methylation status of BNIP3 and BNIP3L by genome sequencing

Methylation of BNIP3 and BNIP3L should be confirmed through complete genome sequencing to overcome limitation of bisulfite sequencing. In the present study, BNIP3 and BNIP3L were not methylated (Fig 3.14B & 3.15). However, use of bisulfite sequencing also has some limitation and it is not sufficient to completely cover CpG island, which is longer than 400bp[121]. Because DNA fragmentation can occur during the bisulfite treatment, amplicon size for both bisulfite genomic sequencing and pyroassay is limited up to ~400 and 500bp. In addition, the high redundancy of the target sequence due to the original GC richness creates long stretches of thymines, which are often difficult to read for the polymerases. This problem can be overcome by complete genome sequencing through next generation sequencing (NGS) and it may provide conclusive answers for the questions. Using the Illumina sequencing, I foresee that results in this study will be precisely confirmed.

4.1.2. Indirect suppression of BNIP3 and BNIP3L by PI3K/Akt

In the present study, the sequence of unmethylated BNIP3 and BNIP3L showed that direct DNA methylation did not occur (Fig 3.14 & 3.15). As previously mentioned, this methylation should be validated. However, if the validation result does not show that CpG islands of BNIP3 and BNIP3 are not methylated, it is possible to approach this matter with indirect down regulation of BNIP3 by activation of PI3K/Akt pathway. It was reported that NF-κB activation located downstream signaling pathway of PI3K/Akt is crucial for the silencing of BNIP3 through E2F1-dependent gene transcription[114]. Also, we previously reported that activation of PI3K/Akt leads to cell cycle recovery from cell cycle arrest induced by LeTx in human acute monocytic leukemia cell line, THP-1 cell[122]. The linkage between cell cycle recovery via PI3K/Akt activation and toxin induced resistance mechanism by down regulation of BNIP3 & BNIP3L should be examined. It

will provide insight how Akt activation by LeTx leads to activation of NF-κB, resulting in suppression of BNIP3 and BNIP3 in TIR.

4.1.3. Mechanism of recruitment between methylated BNIP3/BNIP3L by DNMT1 & HDAC8

Mechanism showing how DNMT1 and HDAC8 cooperatively act together for suppression of BNIP3 and BNIP3L should be examined in depth. We have found that DNMT1 and HDAC8 are involved in down regulation of BNIP3 and BNIP3L (Fig 3.13, 3.16 & 3.18). We should decipher the underlying mechanism how DNMT1 cooperatively interacts with HDAC8 for the repression of transcription, leading to silence of BNIP3 and BNIP3L. It has been reported that methylated DNA in chromatin binds to the transcription repressor proteins, MeCP2 and MBD2, which in turn recruit histone deacetylase, and forms histone deacetylase complex, leading to repression of genes[94, 95]. For this goal, I suggest that increased expression of MBD and MeCP2 in TIR should be examined using quantitative real time PCR. Also, immunoprecipitation will allow us to examine if methylation of BNIP3 and BNIP3L or other possible cell death genes by DNMT1 in TIR will bind to MeCP2 and MBD2 and subsequently recruits histone deacetylase complex. At the same time, it should be examined that if HDAC8 are recruited to this histone deacetylase complex.

4.1.4. Roles of HDAC8 and HAT for BNIP3/ BNIP3L expressions in histone modification

For histone modification, the present study showed that H3K27Ac as an enhancer was down regulated in TIR, leading to down regulation of BNIP3 based on Western Blot & ChIP assay (Fig 3.18 & 3.19). However, the specific link between HDAC8 and H3K27Ac for histone modification was not yet specifically addressed in this study. Though it was shown that broad spectrum HDAC inhibitor, panobinostat restored expression of H3K27Ac (Fig 3.18), we should also conduct further experiment to determine if specific knock down of HDAC8 will lead to expression of H3K27Ac. In addition, since BNIP3L expression was not affected by H3K27Ac, we should further examine that BNIP3L expression was affected by other histone modification enhancers such as H3K79Ac and H3K36Ac or histone methylation of H3K4me.

We also found that other histone deacetylase 9 (HDAC9) showed a 2.5 fold increase in TIR (Fig 3.8). In this study, we examined only HDAC8, which showed highest expression. However, we should examine if expressions of HDAC9 is correlated with resistance of TIR. If so, we should further examine if HDAC9 down regulates BNIP3 and BNIP3L.

In terms of histone acetyl transferase (HAT), it is elusive if TIR cells will gain sensitivity through HAT, leading to up-regulation of BNIP3 and BNIP3L. Therefore, we should examine if acetylation of H3K27 by CBP (CREB binding protein)/ P300 protein which has intrinsic histone acetyltransferase activity, will subsequently lead to increased expression of BNIP3 and BNIP3L in TIR (Fig 4.1).

4.1.5. Effect of histone methylation on BNIP3/BNIP3L expression

Histone methylation is the modification of certain amino acids such as Lysine or Arginine in a histone protein by addition of one, two, or three methyl groups[123]. Histone methylation induces either transcriptional repression or activation. It was shown that trimethylation of lysines (K) positioned on 4, 36, or 79 on H3 (H3K4me3, H3K36me3, and H3K79me3, respectively), monomethylation of H4K20 and H2K5 (H4K20me and H2BK5me) result in gene activation, whereas di- or trimethylation of H3K9 (H3K9me2 and H3K9me3) and H3K27 (H3K27me3) lead to gene repression[82, 85]. Trimethylation of H3K4 (H3K4me3) was identified in BNIP3L through ENCODE site and it may lead to activation of BNIP3L; Activation of H3K4me3 may lead to restoration of down regulated BNIP3L by HDAC8. Further ChIP assay and Western blot will allow us to examine if expression of BNIP3 and BNIP3L are affected by histone methylation.

4.2. Therapeutic potential

For the treatment of Anthrax, current therapy is limited to antibiotics such as ciprofloxacin or doxycycline. In addition, the antibiotic treatment cannot be effective in the case of inhalation infection; it can be 45% lethal even with treatment of antibiotics. Though anthrax vaccine is available in the U.S military against bioterrorism, the vaccine use for public is limited. Because it should be administered four times per year accompanying with an annual booster, this can be a complicated procedure for patients

and because of that, it can cause delay in the immunization schedule. At this moment, it is not clear whether inducing TIR in macrophages or other cells is beneficial for the host in anthrax. NLRP1b was shown to be required for early detection *B. anthracis* and preventing anthrax in a mouse *B. anthracis* spore infection model[40]. The beneficial effect of NLRP1b is likely due to early release of IL-1β and IL-18, which induces early inflammatory responses during infection. However, in situations when antibiotics are already in place, overt inflammation may not be beneficial for the host and thus preventing NLRP1b activation could be beneficial. In addition, LeTx can be detrimental to host considering that LeTx enhances dissemination of bacteria beyond the draining lymphoid tissue, which could be mediated through pyroptosis. It was also shown that LeTx-induced cytotoxicity in mice and rats is detrimental for the hosts[33, 124]. Therefore, tailed therapies, preventing pyroptosis without affecting the IL-1β and IL-18, could be an ideal approach for treating anthrax. Further studies elucidating the mechanism specific for pyroptosis will provide new opportunities for developing novel interventions for anthrax.

REFERENCES

1. Hanna, P. Anthrax pathogenesis and host response. *Curr. Top. Microbiol. Immunol.* **225**, 13-35 (1998).

2. Tournier, J. N., Quesnel-Hellmann, A., Cleret, A. & Vidal, D. R. Contribution of toxins to the pathogenesis of inhalational anthrax. *Cell. Microbiol.* **9**, 555-565 (2007).

3. Guidi-Rontani, C., Levy, M., Ohayon, H. & Mock, M. Fate of germinated Bacillus anthracis spores in primary murine macrophages. *Mol. Microbiol.* **42**, 931-938 (2001).

4. Steelfisher, G. K. *et al*. Public Response to an Anthrax Attack: A Multiethnic Perspective. *Biosecur Bioterror* **10**, 401-411 (2012).

5. Dragon, D. C., Rennie, R. P. & Elkin, B. T. Detection of anthrax spores in endemic regions of northern Canada. *J. Appl. Microbiol.* **91**, 435-441 (2001).

6. Dragon, D. C. & Rennie, R. P. The ecology of anthrax spores: tough but not invincible. *Can. Vet. J.* **36**, 295-301 (1995).

7. http://www.cbc.ca/news/canada/saskatchewan/story/2006/07/18/anthrax.html.

8. Brossier, F. & Mock, M. Toxins of Bacillus anthracis. *Toxicon* **39**, 1747-1755 (2001).

9. Boyer, A. E. *et al*. Lethal factor toxemia and anti-protective antigen antibody activity in naturally acquired cutaneous anthrax. *J. Infect. Dis.* **204**, 1321-1327 (2011).

10. Holty, J. E. *et al*. Systematic review: a century of inhalational anthrax cases from 1900 to 2005. *Ann. Intern. Med.* **144**, 270-280 (2006).

11. LaForce, F. M. Anthrax. *Clin. Infect. Dis.* **19**, 1009-13; quiz 1014 (1994).

12. Sirisanthana, T., Navachareon, N., Tharavichitkul, P., Sirisanthana, V. & Brown, A. E. Outbreak of oral-oropharyngeal anthrax: an unusual manifestation of human infection with Bacillus anthracis. *Am. J. Trop. Med. Hyg.* **33**, 144-150 (1984).

13. Sirisanthana, T., Nelson, K. E., Ezzell, J. W. & Abshire, T. G. Serological studies of patients with cutaneous and oral-oropharyngeal anthrax from northern Thailand. *Am. J. Trop. Med. Hyg.* **39**, 575-581 (1988).

14. Ribot, W. J. *et al*. Anthrax lethal toxin impairs innate immune functions of alveolar macrophages and facilitates Bacillus anthracis survival. *Infect. Immun.* **74**, 5029-5034 (2006).

15. Abramova, F. A., Grinberg, L. M., Yampolskaya, O. V. & Walker, D. H. Pathology of inhalational anthrax in 42 cases from the Sverdlovsk outbreak of 1979. *Proc. Natl. Acad. Sci. U. S. A.* **90**, 2291-2294 (1993).

16. Quinn, C. P. *et al*. A three-dose intramuscular injection schedule of anthrax vaccine adsorbed generates sustained humoral and cellular immune responses to protective antigen and provides long-term protection against inhalation anthrax in rhesus macaques. *Clin. Vaccine Immunol.* **19**, 1730-1745 (2012).

17. Stephanie Yao. **FDA approves raxibacumab to treat inhalational anthrax**. *FDA NEWS RELEASE* (Dec 2012).

18. Abrami, L., Liu, S., Cosson, P., Leppla, S. H. & van der Goot, F. G. Anthrax toxin triggers endocytosis of its receptor via a lipid raft-mediated clathrin-dependent process. *J. Cell Biol.* **160**, 321-328 (2003).

19. Collier, R. J. & Young, J. A. Anthrax toxin. *Annu. Rev. Cell Dev. Biol.* **19**, 45-70 (2003).

20. Bradley, K. A. *et al*. Binding of anthrax toxin to its receptor is similar to alpha integrin-ligand interactions. *J. Biol. Chem.* **278**, 49342-49347 (2003).

21. Bradley, K. A. & Young, J. A. Anthrax toxin receptor proteins. *Biochem. Pharmacol.* **65**, 309-314 (2003).

22. Abrami, L., Reig, N. & van der Goot, F. G. Anthrax toxin: the long and winding road that leads to the kill. *Trends Microbiol.* **13**, 72-78 (2005).

23. Mock, M. & Fouet, A. Anthrax. *Annu. Rev. Microbiol.* **55**, 647-671 (2001).

24. Leppla, S. H. Anthrax toxin edema factor: a bacterial adenylate cyclase that increases cyclic AMP concentrations of eukaryotic cells. *Proc. Natl. Acad. Sci. U. S. A.* **79**, 3162-3166 (1982).

25. Montecucco, C., Tonello, F. & Zanotti, G. Stop the killer: how to inhibit the anthrax lethal factor metalloprotease. *Trends Biochem. Sci.* **29**, 282-285 (2004).

26. Baldari, C. T., Tonello, F., Paccani, S. R. & Montecucco, C. Anthrax toxins: A paradigm of bacterial immune suppression. *Trends Immunol.* **27**, 434-440 (2006).

27. Campbell, S. L., Khosravi-Far, R., Rossman, K. L., Clark, G. J. & Der, C. J. Increasing complexity of Ras signaling. *Oncogene* **17**, 1395-1413 (1998).

28. Kyriakis, J. M. & Avruch, J. Mammalian mitogen-activated protein kinase signal transduction pathways activated by stress and inflammation. *Physiol. Rev.* **81**, 807-869 (2001).

29. Cuenda, A. & Rousseau, S. p38 MAP-kinases pathway regulation, function and role in human diseases. *Biochim. Biophys. Acta* **1773**, 1358-1375 (2007).

30. Madhani, H. D. & Fink, G. R. The riddle of MAP kinase signaling specificity. *Trends Genet.* **14**, 151-155 (1998).

31. Kim, S. O. *et al*. Sensitizing anthrax lethal toxin-resistant macrophages to lethal toxin-induced killing by tumor necrosis factor-alpha. *J. Biol. Chem.* **278**, 7413-7421 (2003).

32. Ivins, B. E. & Welkos, S. L. Cloning and expression of the Bacillus anthracis protective antigen gene in Bacillus subtilis. *Infect. Immun.* **54**, 537-542 (1986).

33. Boyden, E. D. & Dietrich, W. F. Nalp1b controls mouse macrophage susceptibility to anthrax lethal toxin. *Nat. Genet.* **38**, 240-244 (2006).

34. Meylan, E., Tschopp, J. & Karin, M. Intracellular pattern recognition receptors in the host response. *Nature* **442**, 39-44 (2006).

35. Martinon, F., Mayor, A. & Tschopp, J. The inflammasomes: guardians of the body. *Annu. Rev. Immunol.* **27**, 229-265 (2009).

36. Martinon, F. Signaling by ROS drives inflammasome activation. *Eur. J. Immunol.* **40**, 616-619 (2010).

37. Franchi, L., Munoz-Planillo, R. & Nunez, G. Sensing and reacting to microbes through the inflammasomes. *Nat. Immunol.* **13**, 325-332 (2012).

38. Gross, O., Thomas, C. J., Guarda, G. & Tschopp, J. The inflammasome: an integrated view. *Immunol. Rev.* **243**, 136-151 (2011).

39. Frew, B. C., Joag, V. R. & Mogridge, J. Proteolytic processing of Nlrp1b is required for inflammasome activity. *PLoS Pathog.* **8**, e1002659 (2012).

40. Moayeri, M. *et al*. Inflammasome sensor Nlrp1b-dependent resistance to anthrax is mediated by caspase-1, IL-1 signaling and neutrophil recruitment. *PLoS Pathog.* **6**, e1001222 (2010).

41. Lamkanfi, M. & Dixit, V. M. Modulation of inflammasome pathways by bacterial and viral pathogens. *J. Immunol.* **187**, 597-602 (2011).

42. Moayeri, M. & Leppla, S. H. Cellular and systemic effects of anthrax lethal toxin and edema toxin. *Mol. Aspects Med.* **30**, 439-455 (2009).

43. Brennan, M. A. & Cookson, B. T. Salmonella induces macrophage death by caspase-1-dependent necrosis. *Mol. Microbiol.* **38**, 31-40 (2000).

44. Cervantes, J., Nagata, T., Uchijima, M., Shibata, K. & Koide, Y. Intracytosolic Listeria monocytogenes induces cell death through caspase-1 activation in murine macrophages. *Cell. Microbiol.* **10**, 41-52 (2008).

45. Fink, S. L., Bergsbaken, T. & Cookson, B. T. Anthrax lethal toxin and Salmonella elicit the common cell death pathway of caspase-1-dependent pyroptosis via distinct mechanisms. *Proc. Natl. Acad. Sci. U. S. A.* **105**, 4312-4317 (2008).

46. Fernandes-Alnemri, T. *et al*. The pyroptosome: a supramolecular assembly of ASC dimers mediating inflammatory cell death via caspase-1 activation. *Cell Death Differ.* **14**, 1590-1604 (2007).

47. Fink, S. L. & Cookson, B. T. Apoptosis, pyroptosis, and necrosis: mechanistic description of dead and dying eukaryotic cells. *Infect. Immun.* **73**, 1907-1916 (2005).

48. Fink, S. L. & Cookson, B. T. Caspase-1-dependent pore formation during pyroptosis leads to osmotic lysis of infected host macrophages. *Cell. Microbiol.* **8**, 1812-1825 (2006).

49. Alileche, A., Squires, R. C., Muehlbauer, S. M., Lisanti, M. P. & Brojatsch, J. Mitochondrial impairment is a critical event in anthrax lethal toxin-induced cytolysis of murine macrophages. *Cell. Cycle* **5**, 100-106 (2006).

50. Ha, S. D. *et al*. Mitochondrial proteins Bnip3 and Bnip3L are involved in anthrax lethal toxin-induced macrophage cell death. *J. Biol. Chem.* **282**, 26275-26283 (2007).

51. Averette, K. M. *et al*. Anthrax lethal toxin induced lysosomal membrane permeabilization and cytosolic cathepsin release is Nlrp1b/Nalp1b-dependent. *PLoS One* **4**, e7913 (2009).

52. Bhatnagar, R., Singh, Y., Leppla, S. H. & Friedlander, A. M. Calcium is required for the expression of anthrax lethal toxin activity in the macrophagelike cell line J774A.1. *Infect. Immun.* **57**, 2107-2114 (1989).

53. Shin, S. *et al*. Intracellular calcium antagonist protects cultured peritoneal macrophages against anthrax lethal toxin-induced cytotoxicity. *Cell Biol. Toxicol.* **16**, 137-144 (2000).

54. Hanna, P. C., Kruskal, B. A., Ezekowitz, R. A., Bloom, B. R. & Collier, R. J. Role of macrophage oxidative burst in the action of anthrax lethal toxin. *Mol. Med.* **1**, 7-18 (1994).

55. Ha, S. D., Park, S., Han, C. Y., Nguyen, M. L. & Kim, S. O. Cellular adaptation to anthrax lethal toxin-induced mitochondrial cholesterol enrichment, hyperpolarization, and reactive oxygen species generation through downregulating MLN64 in macrophages. *Mol. Cell. Biol.* **32**, 4846-4860 (2012).

56. Boyd, J. M. *et al*. Adenovirus E1B 19 kDa and Bcl-2 proteins interact with a common set of cellular proteins. *Cell* **79**, 341-351 (1994).

57. Chen, G. *et al*. The E1B 19K/Bcl-2-binding protein Nip3 is a dimeric mitochondrial protein that activates apoptosis. *J. Exp. Med.* **186**, 1975-1983 (1997).

58. Kubli, D. A., Ycaza, J. E. & Gustafsson, A. B. Bnip3 mediates mitochondrial dysfunction and cell death through Bax and Bak. *Biochem. J.* **405**, 407-415 (2007).

59. Guo, K. *et al*. Hypoxia induces the expression of the pro-apoptotic gene BNIP3. *Cell Death Differ.* **8**, 367-376 (2001).

60. Harris, A. L. Hypoxia--a key regulatory factor in tumour growth. *Nat. Rev. Cancer.* **2**, 38-47 (2002).

61. Kubasiak, L. A., Hernandez, O. M., Bishopric, N. H. & Webster, K. A. Hypoxia and acidosis activate cardiac myocyte death through the Bcl-2 family protein BNIP3. *Proc. Natl. Acad. Sci. U. S. A.* **99**, 12825-12830 (2002).

62. Crow, M. T. Hypoxia, BNip3 proteins, and the mitochondrial death pathway in cardiomyocytes. *Circ. Res.* **91**, 183-185 (2002).

63. Marzo, I. *et al*. Bax and adenine nucleotide translocator cooperate in the mitochondrial control of apoptosis. *Science* **281**, 2027-2031 (1998).

64. Daido, S. *et al*. Pivotal role of the cell death factor BNIP3 in ceramide-induced autophagic cell death in malignant glioma cells. *Cancer Res.* **64**, 4286-4293 (2004).

65. Hamacher-Brady, A. *et al*. Response to myocardial ischemia/reperfusion injury involves Bnip3 and autophagy. *Cell Death Differ.* **14**, 146-157 (2007).

66. Bellot, G. *et al*. Hypoxia-induced autophagy is mediated through hypoxia-inducible factor induction of BNIP3 and BNIP3L via their BH3 domains. *Mol. Cell. Biol.* **29**, 2570-2581 (2009).

67. Murai, M. *et al*. Aberrant methylation and silencing of the BNIP3 gene in colorectal and gastric cancer. *Clin. Cancer Res.* **11**, 1021-1027 (2005).

68. Murai, M. *et al*. Aberrant DNA methylation associated with silencing BNIP3 gene expression in haematopoietic tumours. *Br. J. Cancer* **92**, 1165-1172 (2005).

69. Salles, I. I., Tucker, A. E., Voth, D. E. & Ballard, J. D. Toxin-induced resistance in Bacillus anthracis lethal toxin-treated macrophages. *Proc. Natl. Acad. Sci. U. S. A.* **100**, 12426-12431 (2003).

70. Bird, A. Perceptions of epigenetics. *Nature* **447**, 396-398 (2007).

71. Walsh, C. P. & Bestor, T. H. Cytosine methylation and mammalian development. *Genes Dev.* **13**, 26-34 (1999).

72. Bestor, T. H. The DNA methyltransferases of mammals. *Hum. Mol. Genet.* **9**, 2395-2402 (2000).

73. Bird, A. Molecular biology. Methylation talk between histones and DNA. *Science* **294**, 2113-2115 (2001).

74. Feinberg, A. P. Phenotypic plasticity and the epigenetics of human disease. *Nature* **447**, 433-440 (2007).

75. Jones, P. A. & Baylin, S. B. The epigenomics of cancer. *Cell* **128**, 683-692 (2007).

76. Pradhan, S., Bacolla, A., Wells, R. D. & Roberts, R. J. Recombinant human DNA (cytosine-5) methyltransferase. I. Expression, purification, and comparison of de novo and maintenance methylation. *J. Biol. Chem.* **274**, 33002-33010 (1999).

77. Dhe-Paganon, S., Syeda, F. & Park, L. DNA methyl transferase 1: regulatory mechanisms and implications in health and disease. *Int. J. Biochem. Mol. Biol.* **2**, 58-66 (2011).

78. Jones, P. A. & Baylin, S. B. The fundamental role of epigenetic events in cancer. *Nat. Rev. Genet.* **3**, 415-428 (2002).

79. Cameron, E. E., Bachman, K. E., Myohanen, S., Herman, J. G. & Baylin, S. B. Synergy of demethylation and histone deacetylase inhibition in the re-expression of genes silenced in cancer. *Nat. Genet.* **21**, 103-107 (1999).

80. Roth, S. Y., Denu, J. M. & Allis, C. D. Histone acetyltransferases. *Annu. Rev. Biochem.* **70**, 81-120 (2001).

81. Vaquero, A., Loyola, A. & Reinberg, D. The constantly changing face of chromatin. *Sci. Aging Knowledge Environ.* **2003**, RE4 (2003).

82. Kouzarides, T. Chromatin modifications and their function. *Cell* **128**, 693-705 (2007).

83. Chi, P., Allis, C. D. & Wang, G. G. Covalent histone modifications--miswritten, misinterpreted and mis-erased in human cancers. *Nat. Rev. Cancer.* **10**, 457-469 (2010).

84. Li, B., Carey, M. & Workman, J. L. The role of chromatin during transcription. *Cell* **128**, 707-719 (2007).

85. Martin, C. & Zhang, Y. The diverse functions of histone lysine methylation. *Nat. Rev. Mol. Cell Biol.* **6**, 838-849 (2005).

86. Struhl, K. Histone acetylation and transcriptional regulatory mechanisms. *Genes Dev.* **12**, 599-606 (1998).

87. Allis, C. D. & Muir, T. W. Spreading chromatin into chemical biology. *Chembiochem* **12**, 264-279 (2011).

88. Brownell, J. E. & Allis, C. D. Special HATs for special occasions: linking histone acetylation to chromatin assembly and gene activation. *Curr. Opin. Genet. Dev.* **6**, 176-184 (1996).

89. Dhalluin, C. *et al*. Structure and ligand of a histone acetyltransferase bromodomain. *Nature* **399**, 491-496 (1999).

90. Dhalluin, C. *et al*. 1H, 15N and 13C resonance assignments for the bromodomain of the histone acetyltransferase P/CAF. *J. Biomol. NMR* **14**, 291-292 (1999).

91. Grunstein, M. Histone acetylation in chromatin structure and transcription. *Nature* **389**, 349-352 (1997).

92. Bjerling, P. *et al*. Functional divergence between histone deacetylases in fission yeast by distinct cellular localization and in vivo specificity. *Mol. Cell. Biol.* **22**, 2170-2181 (2002).

93. Fischle, W. *et al*. Enzymatic activity associated with class II HDACs is dependent on a multiprotein complex containing HDAC3 and SMRT/N-CoR. *Mol. Cell* **9**, 45-57 (2002).

94. Jones, P. L. *et al*. Methylated DNA and MeCP2 recruit histone deacetylase to repress transcription. *Nat. Genet.* **19**, 187-191 (1998).

95. Wade, P. A. *et al*. Mi-2 complex couples DNA methylation to chromatin remodelling and histone deacetylation. *Nat. Genet.* **23**, 62-66 (1999).

96. Santini, V., Kantarjian, H. M. & Issa, J. P. Changes in DNA methylation in neoplasia: pathophysiology and therapeutic implications. *Ann. Intern. Med.* **134**, 573-586 (2001).

97. Escher, G. *et al*. Demethylation using the epigenetic modifier, 5-azacytidine, increases the efficiency of transient transfection of macrophages. *J. Lipid Res.* **46**, 356-365 (2005).

98. Lemoine, M. *et al*. The pan-deacetylase inhibitor panobinostat induces cell death and synergizes with everolimus in Hodgkin lymphoma cell lines. *Blood* **119**, 4017-4025 (2012).

99. Sung, V. *et al*. Histone deacetylase inhibitor MGCD0103 synergizes with gemcitabine in human pancreatic cells. *Cancer. Sci.* **102**, 1201-1207 (2011).

100. Deng, J. *et al*. Targeted bisulfite sequencing reveals changes in DNA methylation associated with nuclear reprogramming. *Nat. Biotechnol.* **27**, 353-360 (2009).

101. Li, L. C. & Dahiya, R. MethPrimer: designing primers for methylation PCRs. *Bioinformatics* **18**, 1427-1431 (2002).

102. Mikeska, T., Felsberg, J., Hewitt, C. A. & Dobrovic, A. Analysing DNA methylation using bisulphite pyrosequencing. *Methods Mol. Biol.* **791**, 33-53 (2011).

103. Uhlmann, K., Brinckmann, A., Toliat, M. R., Ritter, H. & Nurnberg, P. Evaluation of a potential epigenetic biomarker by quantitative methyl-single nucleotide polymorphism analysis. *Electrophoresis* **23**, 4072-4079 (2002).

104. Colella, S., Shen, L., Baggerly, K. A., Issa, J. P. & Krahe, R. Sensitive and quantitative universal Pyrosequencing methylation analysis of CpG sites. *BioTechniques* **35**, 146-150 (2003).

105. Tusnady, G. E., Simon, I., Varadi, A. & Aranyi, T. BiSearch: primer-design and search tool for PCR on bisulfite-treated genomes. *Nucleic Acids Res.* **33**, e9 (2005).

106. http://www.ncbi.nlm.nih.gov/epigenomics/view/genome/12176/?term=Bnip3.

107. http://genome.ucsc.edu/ENCODE/.

108. Rosenfeld, J. A. *et al*. Determination of enriched histone modifications in non-genic portions of the human genome. *BMC Genomics* **10**, 143-2164-10-143 (2009).

109. Raymond, B. *et al*. Anthrax lethal toxin impairs IL-8 expression in epithelial cells through inhibition of histone H3 modification. *PLoS Pathog.* **5**, e1000359 (2009).

110. Popov, S. G. *et al*. Effect of Bacillus anthracis lethal toxin on human peripheral blood mononuclear cells. *FEBS Lett.* **527**, 211-215 (2002).

111. Van den Wyngaert, I. *et al*. Cloning and characterization of human histone deacetylase 8. *FEBS Lett.* **478**, 77-83 (2000).

112. Gao, S. M. *et al*. Histone deacetylases inhibitor sodium butyrate inhibits JAK2/STAT signaling through upregulation of SOCS1 and SOCS3 mediated by HDAC8 inhibition in myeloproliferative neoplasms. *Exp. Hematol.* (2012).

113. Gang, H. *et al*. Epigenetic regulation of E2F-1-dependent Bnip3 transcription and cell death by nuclear factor-kappaB and histone deacetylase-1. *Pediatr. Cardiol.* **32**, 263-266 (2011).

114. Shaw, J. *et al*. Antagonism of E2F-1 regulated Bnip3 transcription by NF-kappaB is essential for basal cell survival. *Proc. Natl. Acad. Sci. U. S. A.* **105**, 20734-20739 (2008).

115. Barnes, P. J., Adcock, I. M. & Ito, K. Histone acetylation and deacetylation: importance in inflammatory lung diseases. *Eur. Respir. J.* **25**, 552-563 (2005).

116. Zhou, Q., Agoston, A. T., Atadja, P., Nelson, W. G. & Davidson, N. E. Inhibition of histone deacetylases promotes ubiquitin-dependent proteasomal degradation of DNA methyltransferase 1 in human breast cancer cells. *Mol. Cancer. Res.* **6**, 873-883 (2008).

117. Du, Z. *et al*. DNMT1 stability is regulated by proteins coordinating deubiquitination and acetylation-driven ubiquitination. *Sci. Signal.* **3**, ra80 (2010).

118. Ellis, L., Atadja, P. W. & Johnstone, R. W. Epigenetics in cancer: targeting chromatin modifications. *Mol. Cancer. Ther.* **8**, 1409-1420 (2009).

119. Koch, C. M. *et al*. The landscape of histone modifications across 1% of the human genome in five human cell lines. *Genome Res.* **17**, 691-707 (2007).

120. Kondo, Y., Shen, L. & Issa, J. P. Critical role of histone methylation in tumor suppressor gene silencing in colorectal cancer. *Mol. Cell. Biol.* **23**, 206-215 (2003).

121. Grunau, C., Clark, S. J. & Rosenthal, A. Bisulfite genomic sequencing: systematic investigation of critical experimental parameters. *Nucleic Acids Res.* **29**, E65-5 (2001).

122. Ha, S. D., Ng, D., Pelech, S. L. & Kim, S. O. Critical role of the phosphatidylinositol 3-kinase/Akt/glycogen synthase kinase-3 signaling pathway in recovery from anthrax lethal toxin-induced cell cycle arrest and MEK cleavage in macrophages. *J. Biol. Chem.* **282**, 36230-36239 (2007).

123. Zhang, Y. & Reinberg, D. Transcription regulation by histone methylation: interplay between different covalent modifications of the core histone tails. *Genes Dev.* **15**, 2343-2360 (2001).

124. Watson, L. E. *et al*. Anthrax toxins induce shock in rats by depressed cardiac ventricular function. *PLoS One* **2**, e466 (2007).

CURRICULUM VITAE

Name: CHAE YOUNG HAN

Post-secondary   M.Sc. Microbiology & Immunology
Education and   University of Western Ontario
Degrees: London, Ontario, Canada
                   2011-2013 M.Sc.

                   B.S. Biology & Chemistry
                   University of Illinois at Urbana Champaign
                   Urbana, Illinois, USA
                   2002-2005 B.S.

Honors and   Schulich Graduate & Western Graduate Research Scholarships
Awards: 2011-2013

Related Work   Clinical Safety Associate
Experience   Novartis Korea, Seoul, Korea
                   2010 – 2011

                   Regulatory Affairs Associate
                   Hanmi Pharmaceutical Company, Seoul, Korea
                   2008 – 2010

Publications:

Ha, S. D., Park, S., **Han, C. Y.,** Nguyen, M. L. & Kim, S. O. Cellular adaptation to anthrax lethal toxin-induced mitochondrial cholesterol enrichment, hyperpolarization, and reactive oxygen species generation through downregulating MLN64 in macrophages. *Mol. Cell. Biol.* **32**, 4846-4860 (2012).

Presentations:

Han CY, Ha SD, Cherie Tan, & Kim SO. (Nov. 2012). Cellular adaptation of macrophages to anthrax lethal toxin-induced pyroptosis via epigenetic mechanisms, Infection & Immunity Research Forum University of Western Ontario